J. Mech. Phys. Solids Vol. 40, No. 2, pp. 239–271, 1992.
Printed in Great Britain.

0022-5096/92 $5.00 + 0.00

DISLOCATION NUCLEATION FROM A CRACK TIP: AN ANALYSIS BASED ON THE PEIERLS CONCEPT

JAMES R. RICE

Division of Applied Science and Department of Earth and Planetary Sciences, Harvard University, Cambridge, MA 02138, U.S.A.

(*Received* 15 *August* 1991)

ABSTRACT

DISLOCATION nucleation from a stressed crack tip is analyzed based on the Peierls concept. A periodic relation between shear stress and atomic shear displacement is assumed to hold along the most highly stressed slip plane emanating from a crack tip. This allows some small slip displacement to occur near the tip in response to small applied loading and, with increase in loading, the incipient dislocation configuration becomes unstable and leads to a fully formed dislocation which is driven away from the crack. An exact solution for the loading at that nucleation instability is developed via the J-integral for the case when the crack and slip planes coincide, and an approximate solution is given when they do not. Solutions are also given for emission of dissociated dislocations, especially partial dislocation pairs in fcc crystals. The level of applied stress intensity factors required for dislocation nucleation is shown to be proportional to $\sqrt{\gamma_{us}}$, where γ_{us}, the *unstable stacking* energy, is a new solid state parameter identified by the analysis. It is the maximum energy encountered in the block-like sliding along a slip plane, in the Burgers vector direction, of one half of a crystal relative to the other. Approximate estimates of γ_{us} are summarized and the results are used to evaluate brittle vs ductile response in fcc and bcc metals in terms of the competition between dislocation nucleation and Griffith cleavage at a crack tip. The predictions seem compatible with known behavior and also show that in many cases solids which are predicted to first cleave under pure mode I loading should instead first emit dislocations when that loading includes very small amounts of mode II and III shear. The analysis in this paper also reveals a feature of the near-tip slip distribution corresponding to the saddle point energy configuration for cracks that are loaded below the nucleation threshold, as is of interest for thermal activation.

1. INTRODUCTION

ARMSTRONG (1966) and KELLY *et al.* (1967) advanced the viewpoint of brittle vs ductile response as the competition between Griffith cleavage and plastic shear at a crack tip. RICE and THOMSON (1974) specifically modeled the shear process as the nucleation of a dislocation from a stressed crack tip. The Rice and Thomson approach made use of elasticity solutions for a fully formed dislocation (i.e. a dislocation with slip equal to the Burgers vector **b** of some complete or partial lattice dislocation) and a core cut-off parameter had to be introduced to derive a nucleation criterion. Here, following a suggestion by ARGON (1987), the PEIERLS (1940) concept is used in an analysis of dislocation formation at a crack tip. That is, a periodic relation is assumed to hold between shear stress and sliding displacement along a crystal slip plane emanating from a crack tip, and a solution is then derived for the critical external loading which corresponds to dislocation nucleation.

With the results so derived, there will be no further need for the introduction of the poorly defined core cut-off at a crack tip in analyzing such phenomena. Indeed, the results show that no feature resembling a fully formed dislocation is present at the crack tip prior to the instability; the instability begins a slip event leading to a fully formed dislocation which moves away from the crack tip. Prior to the instability there exists only an incipient dislocation in the form of a nonlinear shear distribution along a slip plane, with maximum deformation equivalent to a slip at the crack tip of generally less than a half of that of the fully formed dislocation. The Peierls concept has also been used in a recent analysis of dislocation nucleation by SCHOECK (1991), started simultaneously with the present analysis. His analysis was somewhat more approximate and did not uncover the exact solution for nucleation within the Peierls framework that is derived here. The results which follow identify a new solid state parameter, denoted γ_{us} and called the *unstable stacking* energy, which characterizes the resistance to dislocation nucleation.

2. DESCRIPTION OF MODEL

Suppose a crack tip intersects one of the possible slip planes in a ductile crystal [Fig. 1(a)]. The question addressed here is that of what loading of the cracked solid suffices to nucleate a dislocation from the tip, assuming that cleavage decohesion does not occur first. By adopting the PEIERLS (1940) concept, the shear stress τ along the slip plane is regarded as a (periodic) function of the slip displacement δ along it. Thus, the problem addressed consists of an externally loaded solid containing a crack with traction-free surfaces, and with the additional boundary condition that the shear traction τ must be a function of the slip displacement δ along a plane of displacement discontinuity emanating from the crack tip. For the moment it is assumed that there is a discontinuity of slip displacement only along that plane. More precise models in which there are discontinuities in both shear and opening displacement (the latter relating to dilatancy of an atomic array during large shear and, also, to the presence of tensile stress σ across the slip plane) are discussed by BELTZ and RICE (1991a, b) and SUN *et al.* (1991a). Hence, if $\mathbf{s}$ and $\mathbf{n}$ are unit vectors in the slip direction and normal to the slip plane, then $\delta = u_s^+ - u_s^-$, where $u_s = \mathbf{s}\cdot\mathbf{u}$; $\mathbf{u}$ is the displacement vector and $+$ and $-$ refer to the two sides of the slip plane with $\mathbf{n}$ pointing from $-$ to $+$. Within the present simplification, other components of $\mathbf{u}$ are continuous. Also, $\tau = n_\alpha \sigma_{\alpha\beta} s_\beta = \sigma_{ns}$, where $\sigma_{\alpha\beta}$ is the stress tensor.

The τ vs δ relation is assumed to have a form like in Fig. 1(b), i.e. a periodic function with period b equal to the Burgers vector of a full dislocation, and with an axis crossing in between, at $b/2$ in lattices with simple symmetry. Ways of estimating the form of the relation, and why it has been drawn with a vertical tangent at $\delta = 0$ and b, are discussed below; adaptations of concepts so as to deal with complex dislocations having stacking faults or anti-phase boundaries are discussed in a later section. WEERTMAN (1981) analyzed a similar model but with the τ vs δ relation in the form of a rectagular wave.

The result to be derived in the paper is that dislocation nucleation occurs under critical crack tip stress intensity factors which scale with $\sqrt{\gamma_{us}}$. Here γ_{us}, the unstable

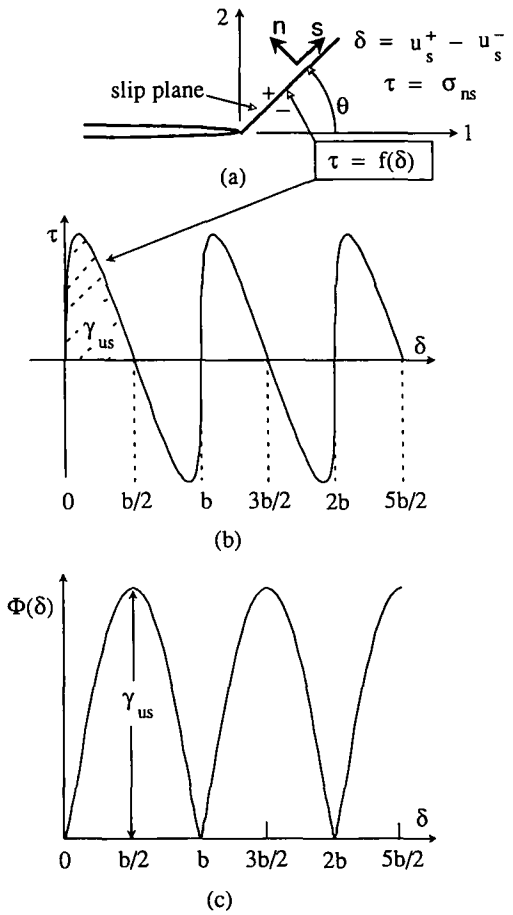

FIG. 1. (a) Crystal slip plane emanating from crack tip. (b) Periodic relation between stress and shear displacement discontinuity (see discussion in connection with Fig. 2 to understand basis for vertical tangent at zero slip). (c) Energy associated with slip discontinuity.

stacking energy, is identified in Fig. 1(b) as the area under the τ vs δ curve between $\delta = 0$ and $\delta = b/2$ (more generally, γ_{us} is the area between $\delta = 0$ and the first δ at which $\tau = 0$ again). Figure 1(c) shows the energy per unit area of the slip plane, $\Phi = \int \tau \, d\delta$. Thus γ_{us} is the maximum value of Φ. One may take the viewpoint that the same τ vs δ relation could be used to describe the block-like shear, along a slip plane, of one half of a perfect lattice relative to the other. Hence Φ (or, more accurately, a related energy Ψ introduced below) corresponds to the γ-energy plot of VITEK (1968) and VITEK *et al.* (1972), and γ_{us}, the maximum value of Φ (and of Ψ) along the slip path, is the energy barrier to be overcome in block-like shear.

To understand the τ vs δ relation, consider the states of shear of an initially rectangular lattice illustrated in Fig. 2. The relative shear displacement of the central pair of planes is denoted Δ; these are separated by distance h and are the pair of

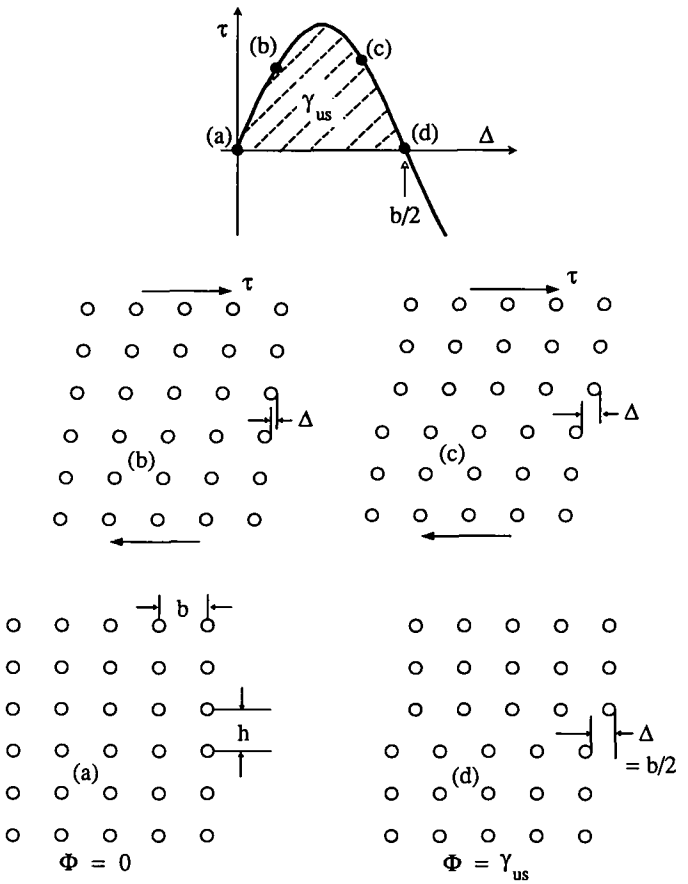

FIG. 2. Various states of shear for a simple cubic lattice; state (d) shows the unstable stacking configuration, with energy γ_{us} per unit area of slip plane.

planes which will ultimately be displaced a lattice distance b. Lattice configurations (a)–(d), starting at the lower left and going clockwise, correspond to points (a)–(d) on the τ vs Δ curve. All the configurations shown are homogeneous in the direction of the shear displacement, but not perpendicular to it. When sufficiently sheared, like in (c) and (d), there exist configurations in which the lattice is not homogeneously strained, like it is in (b), but rather for which the central pair of planes corresponds to a Δ along the descending part of the τ vs Δ relation, while the crystal outside is stressed at the same level at an amount of shear corresponding to the rising part of the curve. Position (d) corresponds to the unstressed but unstable equilibrium state for which the central pair of lattice planes are displaced by $b/2$ while the crystal outside is unstrained. This is the unstable stacking configuration and the work to create it (area under τ vs Δ between $\Delta = 0$ and $b/2$) is γ_{us}, the same γ_{us} of Figs 1(b) and (c), as explained next.

Although the configurations considered in Fig. 2 are homogeneous in the direction of shear, PEIERLS (1940) will be followed in applying the τ vs Δ relation locally to

states of inhomogeneous shear like along the slip plane in Fig. 1(a). Since that inhomogeneous shear is modeled here as a displacement discontinuity, of amount δ, along a cut of zero thickness in an elastic continuum, it is sensible to identify δ not with Δ, which denotes relative displacement of points a distance h apart, but rather to write $\Delta = \delta + h\tau/\mu$ so that relative displacement Δ of atomic planes at spacing h is composed of the discontinuity δ on the mathematical cut plus an additional amount due to elastic shearing by amount τ/μ over a distance h perpendicular to the cut; μ is the shear modulus. Thus, if $\tau = F(\Delta)$, of period b, describes the τ vs Δ relaton of Fig. 2, where $F(0) = 0$ and $\mu = hF'(0)$, then the τ vs δ relation, $\tau = f(\delta)$, is given parametrically by $\tau = F(\Delta)$ and $\delta = \Delta - h\tau/\mu = \Delta - F(\Delta)/F'(0)$. This means that the resulting $\tau = f(\delta)$ is of period b and that $f'(\delta)$ is unbounded at $\delta = 0$, as illustrated in Fig. 1(b). The transformation from Δ to δ as displacement variable preserves the area, namely γ_{us}, under the τ vs displacement curve between the origin and the next zero of τ. An energy $\Psi(\Delta)$ may be defined from $\tau\, d\Delta = d\Psi$; it is the form in which an energy of sheared configurations has been calculated from atomic models [e.g. VITEK (1968), VITEK *et al.* (1972), YAMAGUCHI *et al.* (1981) and SUN *et al.* (1991b)]. Given that the energy $\Phi(\delta)$ of Fig. 1(c) satisfies $\tau\, d\delta = d\Phi$, the relation $\delta = \Delta - h\tau/\mu$ shows that $d\Phi = d\Psi - h\tau\, d\tau/\mu$ and thus that $\Phi(\delta) = \Psi(\Delta) - h\tau^2(\Delta)/2\mu$.

The simplest case of a $\tau = F(\Delta)$ relation is the Frenkel sinusoidal function

$$\tau = (\mu b/2\pi h)\sin(2\pi\Delta/b), \tag{1}$$

in which case

$$\delta = \Delta - (b/2\pi)\sin(2\pi\Delta/b) \tag{2}$$

and the energies Ψ and Φ are

$$\Psi = (\mu b^2/2\pi^2 h)\sin^2(\pi\Delta/b), \quad \Phi = (\mu b^2/2\pi^2 h)\sin^4(\pi\Delta/b). \tag{3}$$

In this case γ_{us}, which is the common maximum of Φ and Ψ, is given by $\gamma_{us} = \mu b^2/2\pi^2 h$, an estimate that will be considered subsequently along with others. The plots in Figs 1(b), 1(c) and 2 have been drawn based on the Frenkel sinusoid. Assuming in general that $\tau = F(\Delta)$ has the series expansion $F(\Delta) = A\Delta - B\Delta^3 + \ldots$ near $\Delta = 0$, with $B \neq 0$, then $\delta = (B/A)\Delta^3 + \ldots$ near $\Delta = 0$, so that the $\tau = f(\delta)$ relation has the form $\delta = B\tau^3/A^4 + \ldots$ near $\tau = 0$. Thus, a vertical tangent of $f(\delta)$ always results at $\delta = 0$.

There seems to be no method of directly measuring γ_{us} other than perhaps by exploiting its significance in the analysis to be developed. However, the type of atomic displacements involved in shifting one half of a crystal relative to the other are relatively simple and susceptible to analysis by atomic models, whether constructed empirically by matching pair or embedded-atom potentials to measured properties (moduli, surface energy, heat of formation, etc.), or found by quantum electronic principles based on density functional theory. Some results based on the former approach are given by SUN *et al.* (1991b).

3. ANALYSIS OF SIMPLIFIED GEOMETRY WITH COINCIDENT CRACK AND SLIP PLANES

While geometries like in Fig. 1(a), typically loaded by tensile, or predominantly tensile, forces relative to the crack plane are of primary interest, the problem posed

is solvable only by numerical methods (BELTZ and RICE, 1991a, b). Tensile loading of that configuration of Fig. 1(a) causes high shear stress τ (at least, when slip δ is precluded) along any slip plane in the general range of, say, $\theta = 30$–$120°$; the mode I crack tip field has highest shear stress along $\theta \approx 70°$. Some of the same features of the configuration of Fig. 1(a), namely, shear along a highly stressed plane emanating from the crack tip, are preserved in the simplified configuration of Fig. 3, for which an exact solution will be derived. In that simplified case, the most stressed slip plane is assumed to be coplanar with the crack ($\theta = 0$), with **s** in the x_1-direction, so emerging dislocations are of edge character relative to the tip, and the external loading is by in-plane (mode II) shear. A nearly identical analysis may be followed when **s** is in the x_3-direction, so that emerging dislocations are of screw type relative to the tip, and loading is by anti-plane shear (mode III).

Along the prolongation of the crack into the slip plane in Fig. 3, $\delta = u_1^+ - u_1^-$ and $\tau = \sigma_{21}$, where $\tau = f(\delta)$ like in Fig. 1(b); u_2 and u_3 are continuous there. Recognizing that this configuration is being analyzed as a simplified analog of more realistic tensile-loaded cases like in Fig. 1(a), the applicability of the τ vs δ relation is not extended back onto the crack faces in Fig. 3 but, rather, it is assumed that the crack faces are traction-free ($\sigma_{2j} = 0$, $j = 1, 2, 3$).

The crack is assumed to be sufficiently long that any region near its tip where significant slip develops, prior to unstable dislocation nucleation, is assumed to be of negligible length compared to crack length and over overall dimensions of the cracked solid, such as distance to boundaries and to points of external force application. In that case it suffices to consider the crack as a semi-infinite slit in an unbounded solid, with all loadings applied at infinitely remote distance so that all that needs to be considered is the singular crack tip stress field, characterized by stress intensity factors, K_I, K_{II} and K_{III}, that the loadings would induce in the linear elastic model of the actual solid. At present, only K_{II} is assumed to be non-zero, such that the stress field ahead of the crack tip ($x_2 = 0, x_1 > 0$) in the linear elastic model of our solid, when restrained

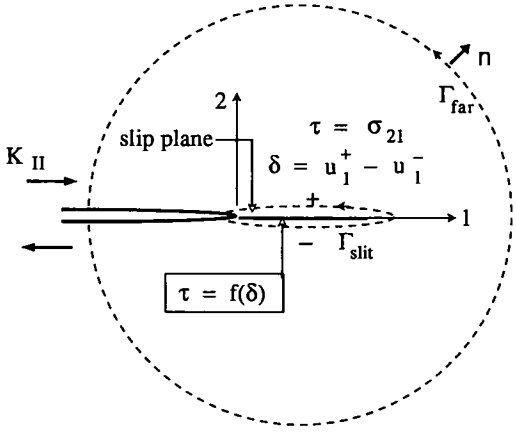

FIG. 3. Coincident crack and slip plane, mode II loading.

against slip δ, is $\sigma_{21} \equiv \tau_o = K_{II}/\sqrt{2\pi r}$, $\sigma_{22} = \sigma_{23} = 0$, with $r = x_1$, and the Irwin energy release rate G is, in the isotropic case,

$$G = (1-\nu)\, K_{II}^2/2\mu, \tag{4}$$

where μ is the shear modulus and ν the Poisson ratio.

A similar argument to that used by RICE (1968a, b) is now followed, based on the path-independent J-integral, in proof of the equivalence of the Griffith criterion $G = 2\gamma_s$ (γ_s = surface energy) for tensile crack growth under mode I loading to the criterion derived from the tensile-decohesion analog of the model described so far here (i.e. from a model in which σ_{22} is a function of opening displacement, $u_2^+ - u_2^-$, along the prolongation of the crack plane, with that function increasing to a maximum and then diminishing to zero at large opening displacements, such that its integral from 0 to ∞ is $2\gamma_s$). That same equivalence was demonstrated earlier by WILLIS (1967), using integral representations of the linear elastic solution for the field outside the decohesion zone, and the Willis method can be adapted to the present analysis of shear dislocation emission at a crack tip. See ESHELBY (1970), RICE (1987) and RICE and WANG (1989) for related discussions.

The J-integral is

$$J = \int_\Gamma [n_1 W(\nabla \mathbf{u}) - n_\alpha \sigma_{\alpha\beta}\, \partial u_\beta/\partial x_1]\, \mathrm{d}s, \tag{5}$$

where W is the strain energy density, $\sigma_{\alpha\beta} = \partial[W(\nabla \mathbf{u})]/\partial(\partial u_\beta/\partial x_\alpha)$ is the stress tensor, s is the arc length, and, here, $\mathbf{n}$ is the unit outward normal to the path Γ, where Γ starts on the lower crack surface, surrounds the crack tip and any slip zone in its vicinity, and ends on the upper crack surface. The integral is independent of path when evaluated for any 2D solution $\mathbf{u}(\mathbf{x})$ of the elastostatic equilibrium equations $\partial \sigma_{\alpha\beta}/\partial x_\alpha = 0$, at least when the elastic properties are invariant to translation in the x_1-direction. The path independence applies not only for conventional stable elastic solutions corresponding to a minimum of the energy functional $U[\mathbf{u}(\mathbf{x})]$, but also to 2D fields $\mathbf{u}(\mathbf{x})$ corresponding to other extremals of $U[\mathbf{u}(\mathbf{x})]$ such as saddle-point configurations, of interest for activation over energy barriers; the field equations $\partial \sigma_{\alpha\beta}/\partial x_\alpha = 0$ are satisfied at all extrema. Here U is the energy of the stressed solid per unit distance along the crack front.

When we assume that the elastic solid outside the slit in Fig. 2 is linear elastic, we may calculate the energy U associated with any solution of the elastic field equations as follows: let U_o be the energy of the loaded elastic solid according to the conventional solution in which δ is constrained to be zero along the slit and the shear stress ahead of the crack is $\tau_o = K_{II}/\sqrt{2\pi r}$. Thus, for the actual slipped configuration, $U[\delta(r)] = U_o$ + the energy of the slip plane due to slip δ + the energy change of the linear system lying outside the slit due to introduction of δ and change of its stress field from τ_o to τ:

$$U[\delta(r)] = U_o + \int_0^\infty \Phi[\delta(r)]\, \mathrm{d}r - \int_0^\infty \tfrac{1}{2}[\tau_o(r) + \tau(r)]\delta(r)\, \mathrm{d}r. \tag{6}$$

Let the functional $s[\delta(r)]$ be the reduction in stress along the line ahead of the crack

due to the introduction of slip $\delta(r)$; $s[\delta(r)]$ corresponds to $\tau_o(r)-\tau(r)$ and is given for the isotropic solid by the principal value integral

$$s[\delta(r)] = \frac{\mu}{2\pi(1-\nu)} \int_0^\infty \sqrt{\frac{\rho}{r}} \frac{\mathrm{d}\delta(\rho)/\mathrm{d}\rho}{r-\rho} \,\mathrm{d}\rho. \tag{7}$$

Thus the energy functional $U[\delta(r)]$ of the loaded cracked body with slip distribution $\delta(r)$ is

$$U[\delta(r)] = U_o + \int_0^\infty \Phi[\delta(r)]\,\mathrm{d}r + \int_0^\infty \tfrac{1}{2} s[\delta(r)]\delta(r)\,\mathrm{d}r - \int_0^\infty \frac{K_{II}}{\sqrt{2\pi r}}\,\delta(r)\,\mathrm{d}r \tag{8}$$

and the problem posed in connection with Figs 3 and 1(b) can be stated as the problem of finding the extrema of this functional. The conditions for such extrema are readily derived (it helps to recall that by elastic reciprocity

$$\int s[\delta_1]\,\delta_2\,\mathrm{d}r = \int s[\delta_2]\,\delta_1\,\mathrm{d}r$$

for any two functions δ_1 and δ_2) and are given by functions $\delta(r)$ satisfying

$$K_{II}/\sqrt{2\pi r} - s[\delta(r)] = \mathrm{d}\Phi[\delta(r)]/\mathrm{d}[\delta(r)]. \tag{9}$$

The left side of (9) is the formula for τ obtained by considering the stresses in the elastic continuum adjoining the slit and the right side is the formula for τ when it is recognized that $\tau = \tau(\delta) \equiv \mathrm{d}\Phi(\delta)/\mathrm{d}\delta$ according to the condition specified on the slit. The numerical solution of such equations is discussed by BELTZ and RICE (1991a, b). Since $\tau \equiv K_{II}/\sqrt{2\pi r} - s[\delta(r)]$ must be finite at $r = 0$, all such solutions meet the condition

$$K_{II} = -\frac{\mu}{\sqrt{2\pi}(1-\nu)} \int_0^\infty \frac{\mathrm{d}\delta(\rho)/\mathrm{d}\rho}{\sqrt{\rho}}\,\mathrm{d}\rho, \tag{10}$$

equivalent to saying that the crack tip is totally shielded by the slip distribution.

Since J has the same value for all paths which do not traverse the crack or slip zone ahead of it, we can advantageously evaluate J on two contours, Γ_{far} and Γ_{slit}; Γ_{far} lies far from the crack tip and the nonlinear perturbation of the linear elastic field due to the incipient slip process near the tip, whereas Γ_{slit} coincides with the upper and lower surfaces of the slit lying ahead of the crack tip on which the displacement u_1 is discontinuous by (variable) amount δ. The value of J on Γ_{far} will depend only on the remote linear elastic field characterized by K_{II} and, as is well known in that case, the result is $J = G$. The value along Γ_{slit} can be written as

$$J = -\int_0^\infty \sigma_{21}\,\partial(u_1^+ - u_1^-)/\partial x_1\,\mathrm{d}x_1 = -\int_0^\infty \tau\,\partial\delta/\partial x_1\,\mathrm{d}x_1 = \int_0^{\delta_{tip}} \tau\,\mathrm{d}\delta \equiv \Phi(\delta_{tip}), \tag{11}$$

where δ_{tip} is the slip displacement discontinuity at the crack tip. Since J is independent

of path, the two evaluations must agree and hence the amount of slip at the crack tip associated with any static solution must satisfy

$$G \equiv (1-\nu)K_{II}^2/2\mu = \Phi(\delta_{tip}). \tag{12}$$

For anisotropic solids the same result applies but with $(1-\nu)/2\mu$ replaced with the appropriate compliance factor from the STROH (1958) and BARNETT and ASARO (1972) results relating G to K_{II}.

Thus as the applied K_{II} and hence G increases from zero, one first follows the rising branch of the $\Phi(\delta)$ function of Fig. 4, having solutions for δ_{tip} like that illustrated at point A. Such δ_{tip} [$= \delta(r)$ at $r = 0$] are reasonably assumed to correspond to functions $\delta(r)$ that give minima of $U[\delta(r)]$ and that represent an incipient, but not yet fully formed, dislocation at the crack tip. It is evident that no static solution can exist when G exceeds γ_{us}, the maximum value of Φ, and hence the incipient dislocation configuration discussed loses stability at

$$G \equiv (1-\nu)K_{II}^2/2\mu = \gamma_{us}, \tag{13}$$

which therefore corresponds to nucleation of a full dislocation. The slip δ_{tip} at the crack tip when instability is reached is well short of that (namely, b) for a full dislocation, and corresponds to $b/2$ in lattices with simple symmetry. Thus no feature resembling a fully formed dislocation is actually present at the crack tip prior to the instability at which the full dislocation is nucleated.

As further shown in Fig. 4, the equation $G = \Phi(\delta_{tip})$ for $G < \gamma_{us}$ has multiple roots, illustrated by solution points A, C, A', A'',.... Points A', A'', etc. have a clear interpretation as corresponding to incipient dislocation configurations after one, two, etc. full dislocations have already been formed from the crack tip. Since A and A' may be presumed to correspond to stable solutions, minimizing $U[\delta(r)]$, it should be expected that there is a saddle-point configuration between these two states, also an extremum of $U[\delta(r)]$. That saddle-point configuration evidently has a slip δ_{tip} at the crack tip given by point C in Fig. 4, and hence we are able to calculate an important feature of the activated configuration, at least in a 2D treatment. This is of limited

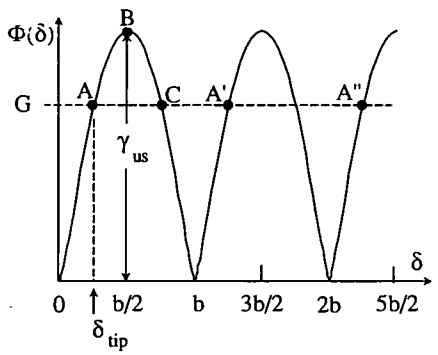

FIG. 4. Solution for the slip displacement at the crack tip, for stable solution A (and A', A'',..., corresponding to one, two, or more previously emitted dislocations), and for 2D saddle-point configuration C.

use because the actual saddle-point configuration, defining the activation energy for an analysis of thermally assisted dislocation nucleation when $G < \gamma_{us}$, will involve a 3D elastic field associated with a localized outward protrusion of slip from the stable 2D incipient dislocation distribution corresponding to point A. Further discussion of activated states in dislocation nucleation is left to later work.

The same analysis as above may be followed for a crack tip loaded under mode III conditions and for which the slip direction **s** is in the x_3-direction, so that the emerging dislocation is of screw type. τ is now identified as σ_{23} and δ as $u_3^+ - u_3^-$. The above equations hold with K_{II} replaced with K_{III}, and with $(1-\nu)$ replaced by 1, so that the nucleation condition is then

$$G \equiv K_{III}^2/2\mu = \gamma_{us}. \tag{14}$$

An alternate derivation of (12), styled on WILLIS' (1967) analysis of the tensile crack, is as follows: the stress at distance r ahead of the crack is $\tau_0(r) - s[\delta(r)]$, or

$$\tau(r) = \frac{K_{II}}{\sqrt{2\pi r}} - \frac{\mu}{2\pi(1-\nu)} \int_0^\infty \sqrt{\frac{\rho}{r}} \frac{\mathrm{d}\delta(\rho)/\mathrm{d}\rho}{r-\rho} \mathrm{d}\rho \tag{15}$$

and the requirement of no singularity at the tip forces K_{II} to be related to an integral involving $\mathrm{d}\delta(\rho)/\mathrm{d}\rho$ as in (10). Using (10), the expression for τ may be written as

$$\tau(r) = -\frac{\mu}{2\pi(1-\nu)} \int_0^\infty \sqrt{\frac{r}{\rho}} \frac{\mathrm{d}\delta(\rho)/\mathrm{d}\rho}{r-\rho} \mathrm{d}\rho \tag{16}$$

so that

$$-\int_0^\infty \tau(r) \frac{\mathrm{d}\delta(r)}{\mathrm{d}r} \mathrm{d}r = \frac{\mu}{2\pi(1-\nu)} \int_{0,0}^{\infty,\infty} \sqrt{\frac{r}{\rho}} \frac{1}{r-\rho} \frac{\mathrm{d}\delta(\rho)}{\mathrm{d}\rho} \frac{\mathrm{d}\delta(r)}{\mathrm{d}r} \mathrm{d}\rho\, \mathrm{d}r. \tag{17}$$

r and ρ can be interchanged in the integrand on the right or, better, the integrand can be replaced by half the form shown plus half of what results when r and ρ are interchanged. Since

$$\frac{1}{2}\sqrt{\frac{r}{\rho}} \frac{1}{r-\rho} + \frac{1}{2}\sqrt{\frac{\rho}{r}} \frac{1}{\rho-r} = \frac{1}{\sqrt{r\rho}}, \tag{18}$$

this shows that

$$-\int_0^\infty \tau(r) \frac{\mathrm{d}\delta(r)}{\mathrm{d}r} \mathrm{d}r = \frac{\mu}{4\pi(1-\nu)} \left(\int_0^\infty \frac{\mathrm{d}\delta(r)/\mathrm{d}r}{\sqrt{r}} \mathrm{d}r \right)^2 = \frac{1-\nu}{2\mu} K_{II}^2, \tag{19}$$

where (10) is used in the last step. Noting now that $\tau = \mathrm{d}\Phi(\delta)/\mathrm{d}\delta$, with $\delta = 0$ at $r = \infty$ and $\delta = \delta_{tip}$ at $r = 0$, this shows that $(1-\nu)K_{II}^2/2\mu = \Phi(\delta_{tip})$, as derived from the J-integral.

As this point, there are three generalizations of the results in need of consideration: (1) How do we deal with the nucleation of general dislocations, combining both edge and screw components, at crack tips under general mixed-mode loading? (2) How do we model the nucleation of dislocations in dissociated form, with first one partial dislocation nucleating, leaving a faulted plane behind it, and then the remainder of

the dislocation nucleating under increased external loading (e.g. fcc metals in which partial dislocations on {111} planes are separated by stacking faults, and ordered alloys in which superlattice dislocations dissociate into partials separated by an anti-phase boundary)? (3) How do we deal with realistic configurations for which the slip plane and the crack plane do not coincide [i.e. $\theta \neq 0$ in Fig. 1(a)]? Reasonably exact results will be derived next for (1) and (2) within a "constrained-path" approximation, that is already tacit in the results presented so far, and then for (3) an approximate procedure will be given for transcribing results derived in the $\theta = 0$ case to cases with $\theta \neq 0$.

4. Results for General Shear Loading, Coincident Crack and Slip Planes

Suppose now that the solid of Fig. 3 is loaded in combined modes I, II and III (Fig. 5) so that stresses on the slip plane in the absence of any relaxation would be $\sigma_{21} = K_{II}/\sqrt{2\pi r}$, $\sigma_{22} = K_I/\sqrt{2\pi r}$ and $\sigma_{23} = K_{III}/\sqrt{2\pi r}$. In general the displacement discontinuity on the slip plane could have components in the 1-, 2- and 3-directions, $\delta_1 = u_1^+ - u_1^-$, $\delta_2 = u_2^+ - u_2^-$ and $\delta_3 = u_3^+ - u_3^-$. The energy $\Phi^*(\delta_1, \delta_2, \delta_3)$ of the slip plane is now related to the stresses by $\sigma_{2\alpha} = \partial\Phi^*(\delta_1, \delta_2, \delta_3)/\partial\delta_\alpha$ and an application of the J-integral paralleling that in the previous section shows that solutions of the static elastic equations for this case must have relative displacements $(\delta_{1tip}, \delta_{2tip}, \delta_{3tip})$ at the crack tip satisfying

$$G \equiv [(1-\nu)(K_I^2 + K_{II}^2) + K_{III}^2]/2\mu = \Phi^*(\delta_{1tip}, \delta_{2tip}, \delta_{3tip}). \tag{20}$$

This condition, however, does not let us determine a nucleation condition since now there are too many degrees of freedom at the tip.

A solution can be found if we make the assumptions that the relative motion along the slip plane is pure shear (so that opening $\delta_2 = 0$), and that a certain direction or more generally that a certain set of crystallographically equivalent directions within a slip plane are far less resistant to shear than are any other directions. Such directions would, of course, coincide with the observed slip directions **s**, i.e. the directions of

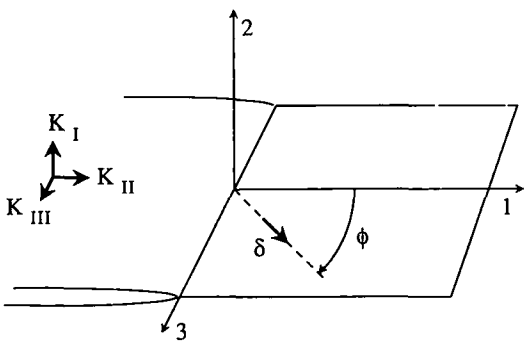

Fig. 5. General mixed-mode loading. Relative displacement along the slip plane assumed to follow a constrained path of pure sliding, without opening, along slip direction at angle ϕ.

Burgers vectors **b**. Calculations from atomic models (YAMAGUCHI *et al.*, 1981; SUN *et al.*, 1991b) of slip plane energies for different directions of shear do indeed show very large differences in energy. Thus let the angle ϕ denote the angle of the easy slip direction on the slip plane, where ϕ is measured from the x_1-axis (Fig. 5) so that $\phi = 0$ corresponds to an edge dislocation, whereas $\phi = \pi/2$ corresponds to a screw dislocation, relative to the crack front. When there are several such directions, we shall regard ϕ as denoting the first such direction to meet the nucleation condition, derived below, under the given ratio of K_{III} to K_{II} loading.

The approximation is now made that the resistance to slip along directions other than ϕ, and the resistance to tensile opening, is so great that the relative displacement can be regarded as being constrained to a pure slip path at angle ϕ, so that

$$\delta_1 = \delta\cos\phi, \quad \delta_2 = 0, \quad \delta_3 = \delta\sin\phi, \tag{21}$$

where δ is the slip along direction ϕ. Thus, if

$$\tau = \sigma_{21}\cos\phi + \sigma_{23}\sin\phi \tag{22}$$

denotes the resolved shear stress in the slip direction, it may be assumed as a boundary condition along the slip plane that τ is related to δ like in Fig. 1(b), and that Φ of Fig. 1(c) is given as before as $\Phi = \int \tau\, d\delta$. Because of the constraint on the relative displacements, it will no longer be the case that the slip process relaxes the stress singularity at the crack tip. Thus, in addition to the K_I, K_{II} and K_{III} characterizing the remotely applied loading, there will also be non-zero stress intensity factors $K_{I(tip)}$, $K_{II(tip)}$ and $K_{III(tip)}$ remaining at the crack tip at $x_1 = 0$.

Evaluation of the J-integral along the path Γ_{far} gives

$$J = G \equiv [(1-\nu)(K_I^2 + K_{II}^2) + K_{III}^2]/2\mu \tag{23}$$

whereas in evaluating the contribution along Γ_{slit} the contribution from the crack tip singularity has to be included now, thus giving

$$\begin{aligned} J &= \{(1-\nu)[K_{I(tip)}^2 + K_{II(tip)}^2] + K_{III(tip)}^2\}/2\mu - \int_0^\infty \sigma_{2\alpha}\,\partial\delta_\alpha/\partial x_1\, dx_1 \\ &= \{(1-\nu)[K_{I(tip)}^2 + K_{II(tip)}^2] + K_{III(tip)}^2\}/2\mu + \Phi(\delta_{tip}), \end{aligned} \tag{24}$$

where it has been noted that $\sigma_{2\alpha}\,\partial\delta_\alpha/\partial x_1 = \tau\,\partial\delta/\partial x_1 = \partial\Phi(\delta)/\partial x_1$ in view of the constraint on the slip path. The following conditions may be brought to bear: since τ is bounded at the tip,

$$K_{II(tip)}\cos\phi + K_{III(tip)}\sin\phi = 0. \tag{25}$$

Using the separate mode I, II and III solutions for the effect of slip on alteration of the stress intensity factors gives

$$\begin{aligned} &[K_I - K_{I(tip)}, K_{II} - K_{II(tip)}, K_{III} - K_{III(tip)}] \\ &\quad = -\frac{\mu}{\sqrt{2\pi}(1-\nu)} \int_0^\infty \frac{d}{d\rho}[\delta_2(\rho), \delta_1(\rho), (1-\nu)\delta_3(\rho)]\,\frac{d\rho}{\sqrt{\rho}}. \end{aligned} \tag{26}$$

When the above constraints on the δ_α are used, this gives

$$K_{I(tip)} = K_I \quad \text{and} \quad (1-\nu)\sin\phi[K_{II}-K_{II(tip)}]-\cos\phi[K_{III}-K_{III(tip)}] = 0. \tag{27}$$

$K_{II(tip)}$ and $K_{III(tip)}$ may therefore be solved as

$$[K_{II(tip)}, K_{III(tip)}] = \frac{(\sin\phi, -\cos\phi)}{\cos^2\phi+(1-\nu)\sin^2\phi}\,[(1-\nu)\sin\phi K_{II}-\cos\phi K_{III}], \tag{28}$$

and when these results are substituted into the two expressions for J above, and the expressions equated, it is found after a little manipulation that the slip δ_{tip} at the crack tip is given by

$$\frac{1-\nu}{2\mu}\,\frac{(\cos\phi K_{II}+\sin\phi K_{III})^2}{\cos^2\phi+(1-\nu)\sin^2\phi} = \Phi(\delta_{tip}). \tag{29}$$

This coincides with the results of the last section for mode II loading in emission of an edge ($\phi = 0$) dislocation and for mode III loading in emission of a screw ($\phi = \pi/2$). Since the maximum of Φ is γ_{us}, the nucleation criterion is therefore

$$\cos\phi K_{II}+\sin\phi K_{III} = \sqrt{\frac{2\mu}{1-\nu}\,[\cos^2\phi+(1-\nu)\sin^2\phi]\gamma_{us}} \tag{30}$$

(assuming that the left side is positive; a minus sign should precede the right side if not). The combination

$$K \equiv \cos\phi K_{II}+\sin\phi K_{III} \tag{31}$$

which enters the criterion has an evident interpretation as the intensity factor for the resolved shear stress along the slip direction.

The combination $[(1-\nu)\sin\phi K_{II}-\cos\phi K_{III}]$ of (28) which gives the strength of the non-relaxed shear stress intensities at the crack tip also has a simple interpretation. Recall that, for the elastic singular field at a crack tip, displacement discontinuities at some small distance r behind the tip are

$$[u_2^+-u_2^-, u_1^+-u_1^-, u_3^+-u_3^-] = \frac{4}{\mu}\sqrt{\frac{r}{2\pi}}\,[(1-\nu)K_I, (1-\nu)K_{II}, K_{III}], \tag{32}$$

so that $(1-\nu)K_I$, $(1-\nu)K_{II}$ and K_{III} may be interpreted as displacement intensity factors. Hence the combination $[(1-\nu)\sin\phi K_{II}-\cos\phi K_{III}]$, to which the non-relaxed shear stress intensity factors are proportional, is just the shear displacement intensity factor resolved in a direction orthogonal to the slip direction. Another interpretation of (27) is that this shear displacement intensity factor retains the same value at the crack tip as it has for the externally applied loading.

It is revealing to manipulate (23) and (24) for J, using (27) and (28), to show that

$$\begin{aligned} G &\equiv [(1-\nu)(K_I^2+K_{II}^2)+K_{III}^2]/2\mu \\ &= \frac{1-\nu}{2\mu}K_I^2+\frac{1}{2\mu}\,\frac{1}{2\mu}\,\frac{[(1-\nu)\sin\phi K_{II}-\cos\phi K_{III}]^2}{\cos^2\phi+(1-\nu)\sin^2\phi}+\Phi(\delta_{tip}), \end{aligned} \tag{33}$$

where the last set of terms involves the unrelaxed displacement intensity factors in tension and orthogonal shear. Indeed, comparing with (20) for the more general case

when the relative displacement is not constrained, it is seen that $\Phi^*(\delta_{1tip}, \delta_{2tip}, \delta_{3tip})$ of the unconstrained treatment exceeds $\Phi(\delta_{tip})$ by the sum of the quadratic terms involving those two unrelaxed intensity factors. The point of view can be taken that the energy Φ^* increases rapidly when the δs deviate from those of the low-energy constrained path, and that the difference between Φ^* and Φ reflects the effect of modest deviations of the δs at the tip from those of the constrained path. The constrained-path approximation made would, presumably, be suspect if the difference between Φ^* and Φ in a given case was much larger than Φ.

Another aspect of the constrained-path approximation is that we really only know, in general, the end points of the path from an undislocated state to a completely dislocated state, at $\delta = b$. It must be expected that, in general, the path actually chosen would deviate along the way from a straight line connecting the endpoints. For example, some tendency for dilatant opening across a lattice plane ($\delta_2 \neq 0$) must, in general, accompany shear, and the shear path itself may have some curvature in the slip plane. A particular embedded-atom model for iron, used in molecular dynamics simulations by CHEUNG (1990), provides an example for which the constrained-path approximation is not so good, in that high tensile stress across slip planes at a crack tip noticeably reduces the resistance to dislocation emission (CHEUNG *et al.*, 1991). These features are important in certain cases, but lie beyond the present level of approximation. They require a more detailed formulation including numerical solution of coupled integral equations for the distribution of the δs; the coupling of dilatant opening and shear has been analyzed based on such numerical solutions in related work by BELTZ and RICE (1991a, b) and SUN *et al.* (1991a) and, for the Cheung *et al.* model of iron, confirm their conclusions. Calculations like those in BELTZ and RICE (1991a, b) show that a reasonable approximation in some cases to the effects of normal stress on shear is to simply identify γ_{us} in (30) as the relaxed value, associated with shear under vanishing σ_{22}. This may be justified as another type of constrained-path approximation, where the δ_2 chosen is that which would correspond to $\sigma_{22} = 0$ along the slip path. We may then derive (30) with the relaxed γ_{us} through a derivation like that above, but with the J-integral in (23) and (24) written exclusively for the shear part of the deformation field.

5. NUCLEATION OF DISSOCIATED DISLOCATIONS, COINCIDENT CRACK AND SLIP PLANES

Suppose that a complete lattice dislocation in a certain crystal is composed of two partial dislocations with respective Burgers vectors $\mathbf{b}_A$ and $\mathbf{b}_B$, where these share the same slip plane and are separated by a faulted portion of slip plane with energy γ_{sf} (*stacking fault* energy) per unit area. The simplification that the crack plane and slip plane are coincident as in Fig. 5 is used and the constrained-path approximation is made for each partial dislocation individually. Thus, partial dislocation A is created by slip δ_A from 0 to b_A along a definite direction at angle ϕ_A (the first of the different possible partial dislocation directions on the slip plane to meet the nucleation condition, under the prevailing K_{III}/K_{II} ratio), and then partial dislocation B can come into existence by slip δ_B from 0 to b_B at angle ϕ_B (taken to be the most favorable of the allowed crystal directions for continuation of slip as a second partial). For {111}

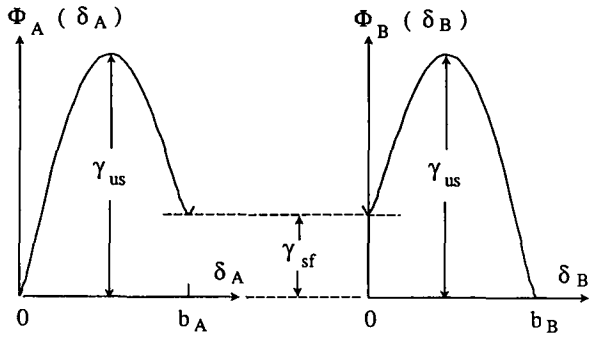

FIG. 6. Energy vs slip for two partial dislocations which combine to form a complete lattice dislocation; γ_{sf} is the energy per unit area of the stacking fault.

planes in fcc lattices, with partials of Burgers vectors in $\langle 211 \rangle$ directions summing to complete $\langle 110 \rangle$ dislocations, ϕ_B and ϕ_A differ by 60°. [ANDERSON (1986) previously analyzed partial dislocation nucleation within the Rice–Thomson framework.]

Energy functions Φ for the two partials are shown in Fig. 6. The first slip over b_A carries the energy Φ_A from zero, through the peak at γ_{us}, and to a residual state of energy γ_{sf}; the next slip starts with energy Φ_B at γ_{sf}, goes through the same peak γ_{us}, and returns to zero after slip b_B, a complete dislocation having then been formed.

Let

$$K_A = K_{II}\cos\phi_A + K_{III}\sin\phi_A, \quad K_B = K_{II}\cos\phi_B + K_{III}\sin\phi_B. \tag{34}$$

The analysis of the previous section shows that the first partial nucleates when

$$K_A = K_{A\text{crit}} \equiv \sqrt{\frac{2\mu}{1-\nu}[\cos^2\phi_A + (1-\nu)\sin^2\phi_A]\gamma_{us}}. \tag{35}$$

However, the fully formed partial dislocation which emerges, of Burgers vector $\mathbf{b}_A$, leaves a faulted plane of energy γ_{sf} behind it and thus is not swept indefinitely far away by the stress field but instead remains in the vicinity of the crack tip. Let r_A be the position of the core of that partial dislocation. It is determined by equilibrium between Peach–Koehler configurational forces; that due to the applied stress field $K_A/\sqrt{2\pi r}$ must balance the sum of the dislocation image force due to the presence of the stress-free crack surface (RICE and THOMSON, 1974) and the force γ_{sf} tending to annihilate the fault. (This defect can be treated as a classical, singular line dislocation, without considering its spread-out core, since it will be seen that r_A is typically very large compared to b_A.) Thus, r_A is the (largest) root of

$$K_A b_A/\sqrt{2\pi r_A} = \gamma_{sf} + \mu b_A^2[\cos^2\phi_A + (1-\nu)\sin^2\phi_A]/4\pi(1-\nu)r_A, \tag{36}$$

from which it is found that

$$\frac{\mu b_A}{(1-\nu)\sqrt{2\pi r_A}} = \frac{K_A[1-\sqrt{1-(\gamma_{sf}/\gamma_{us})(K_{A\text{crit}}/K_A)^2}]}{\cos^2\phi_A + (1-\nu)\sin^2\phi_A} \tag{37}$$

(the combination on the left will be needed shortly) and that

$$\frac{r_A}{b_A} = \frac{(K_{A\text{crit}}/K_A)^2[\cos^2\phi_A + (1-\nu)\sin^2\phi_A](\mu b_A/\gamma_{us})}{4\pi(1-\nu)[1-\sqrt{1-(\gamma_{sf}/\gamma_{us})(K_{A\text{crit}}/K_A)^2}]^2}. \tag{38}$$

The last expression, to be used after nucleation ($K_A \geqslant K_{A\text{crit}}$), defines a rapidly increasing function of K_A. It is least when $K_A = K_{A\text{crit}}$, and then gives the position r_A to which the partial jumps just after nucleation. Later estimates of $\mu b_A/\gamma_{us}$ ranging from 25 to 40 will be seen for fcc metals, and $\gamma_{sf} \approx \gamma_{us}/4$–$\gamma_{us}/2$ seems to be representative (smaller values give larger r_A). These lead, for $\phi_A = 0$ and $\nu = 0.3$, to $r_A/b \approx 30$–250.

The simplest way to address emission of the second partial is to note that the first partial dislocation has the effect of: (i) modifying the K_{II} and K_{III} at the tip (say, to values K_{II}^* and K_{III}^*), and (ii) resetting the energy of the unslipped state from zero to γ_{sf} (Fig. 6) so that the peak energy to be surmounted for the instability leading to dislocation B to occur is reduced from γ_{us} to $\gamma_{us}-\gamma_{sf}$. With those factors taken into account, the result of the last section can just be used so that, at instability

$$K_B^* \equiv K_{II}^*\cos\phi_B + K_{III}^*\sin\phi_B = \sqrt{\frac{2\mu}{1-\nu}[\cos^2\phi_B + (1-\nu)\sin^2\phi_B](\gamma_{us}-\gamma_{sf})}. \tag{39}$$

(When the expressions for K_{II}^* and K_{III}^*, given next, are taken into account, the same result could be derived, alternatively, by applying the J-integral, in the style of the last section, to the entire dislocated array, partial dislocation A, the associated stacking fault zone, and incipient partial dislocation B.)

The expressions for K_{II}^* and K_{III}^* are derivable from (26) as

$$K_{II}^* = K_{II} - \mu b_A\cos\phi_A/(1-\nu)\sqrt{2\pi r_A}, \quad K_{III}^* = K_{III} - \mu b_A\sin\phi_A/\sqrt{2\pi r_A}. \tag{40}$$

Using (37) for the latter terms, the quantity K_B^* entering the criterion for nucleation of the second partial is given by

$$K_B^* = K_B - \eta K_A + \eta\sqrt{K_A^2 - 2\mu\gamma_{sf}[\cos^2\phi_A + (1-\nu)\sin^2\phi_A]/(1-\nu)}, \tag{41}$$

where

$$\eta = \frac{\cos\phi_A\cos\phi_B + (1-\nu)\sin\phi_A\sin\phi_B}{\cos^2\phi_A + (1-\nu)\sin^2\phi_A}. \tag{42}$$

The resulting nucleation criterion is a little complex to study in general, but it takes a simpler form in a special case of considerable interest for fcc metals, in which $\phi_A = 0°$ and $|\phi_B| = 60°$ (+ or − chosen according to the sign of K_{III}). The 0° partial will be the first nucleated only if $K_B < (\sqrt{4-3\nu}/2)K_A$, which is equivalent to $|K_{III}| < (\sqrt{4-3\nu}-1)K_{II}/\sqrt{3}$ or, for $\nu = 0.3$, to $|K_{III}| < 0.44K_{II}$, a condition which is now assumed to hold. The first partial nucleates when

$$K_{II} = \sqrt{2\mu\gamma_{us}/(1-\nu)} \tag{43}$$

and the condition for nucleation of the second, given above, now simplifies to

$$\sqrt{3}\,|K_{III}| + \sqrt{K_{II}^2 - 2\mu\gamma_{sf}/(1-\nu)} = \sqrt{2\mu(4-3\nu)(\gamma_{us}-\gamma_{sf})/(1-\nu)}. \tag{44}$$

Since this equation takes effect only after K_{II} reaches the value to nucleate the first partial, the K_{II} which enters it will always be at least as large as that of (43), and hence the quantity of which the square root is taken is always positive since (since $\gamma_{us} > \gamma_{sf}$).

Three possibilities exist, depending on K_{III}: (i) when K_{III} is zero or sufficiently small, K_{II} must be increased to nucleate the second partial; (ii) for $|K_{III}|$ greater than a certain limit $K_{III(sp)}$ given below, the second partial nucleates spontaneously once the first has formed; no increase in K_{II} is then required; and (iii) for $|K_{III}|$ yet larger, the analysis ultimately becomes untenable because, instead, the $|\phi| = 60°$ partial nucleates first, and we have to start from the beginning, interchanging A and B.

The greatest K_{II} to nucleate the second partial results when $K_{III} = 0$, in which case

$$K_{II} = \sqrt{2\mu[(4-3\nu)\gamma_{us} - 3(1-\nu)\gamma_{sf}]/(1-\nu)}\,. \tag{45}$$

When $\nu = 0.3$ and $\gamma_{sf} = \gamma_{us}/3$, this is 55% higher than the K_{II} to nucleate the first dislocation. The required increase in K_{II} diminishes to zero when $|K_{III}| = K_{III(sp)}$, where

$$K_{III(sp)} = \sqrt{2\mu(\gamma_{us} - \gamma_{sf})/(1-\nu)}\,(\sqrt{4-3\nu} - 1)/\sqrt{3} \tag{46}$$

is calculated by setting K_{II} equal to that to nucleate the first partial. For the numerical values above, $K_{III(sp)}$ is 0.36 times the K_{II} to nucleate the first partial. The range of K_{III} for which there is spontaneous nucleation of the 60° partial persists up to a limit given by the same expression as for $K_{III(sp)}$ but with $(\gamma_{us} - \gamma_{sf})$ increased to γ_{us}; beyond that limit, it is the 60° partial which nucleates first.

Nucleation by the partial mechanism discussed here is considered again in the next section, where slip planes at angle $\theta \neq 0$ are considered.

6. Approximate Nucleation Condition, Slip Plane not Coincident with Crack Plane

In general the most highly stressed slip plane will make a non-zero angle θ relative to the crack plane, like in Fig. 7, and the Burgers vector direction along that plane will make an angle ϕ with a line drawn perpendicular to the crack tip, similar to Fig. 5.

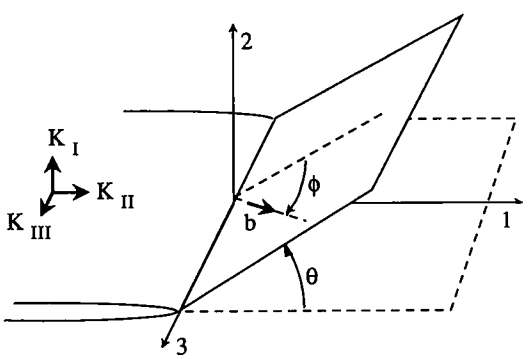

Fig. 7. Slip plane inclined at angle θ with the prolongation of the crack plane; slip direction inclined at angle ϕ with the normal to the crack tip.

Supposing that the solid is loaded so as to induce a general set of intensity factors K_I, K_{II} and K_{III} at the crack tip, the in- and anti-plane shear stress components acting along the slip plane, according to the linear elastic solution, are

$$\sigma_{\theta r} = [K_I f_I(\theta) + K_{II} f_{II}(\theta)]/\sqrt{2\pi r}, \quad \sigma_{\theta 3} = K_{III} f_{III}(\theta)/\sqrt{2\pi r}, \tag{47}$$

where, for the isotropic case,

$$f_I(\theta) = \cos^2(\theta/2)\sin(\theta/2), \quad f_{II}(\theta) = \cos(\theta/2)[1-3\sin^2(\theta/2)], \quad f_{III}(\theta) = \cos(\theta/2). \tag{48}$$

The form of these results motivates the notion of *effective* mode II and mode III intensity factors along the slip plane at angle θ. These are defined as

$$K_{II}^{\text{eff}} = K_I f_I(\theta) + K_{II} f_{II}(\theta), \quad K_{III}^{\text{eff}} = K_{III} f_{III}(\theta). \tag{49}$$

As a simple approximation, it may now be assumed that the nucleation conditions derived for $\theta = 0$ in all the earlier sections of this paper apply as well to an inclined slip plane, $\theta \neq 0$, when K_{II} and K_{III} are replaced in expressions earlier in this paper with the effective intensity factors K_{II}^{eff} and K_{III}^{eff} above. Thus, the basic nucleation condition of (30) for a complete dislocation becomes, approximately when $\theta \neq 0$,

$$[f_I(\theta)K_I + f_{II}(\theta)K_{II}]\cos\phi + f_{III}(\theta)K_{III}\sin\phi = \sqrt{\frac{2\mu}{1-\nu}[\cos^2\phi + (1-\nu)\sin^2\phi]\gamma_{us}} \tag{50}$$

and corresponding results are given shortly for nucleation of a dissociated dislocation.

For pure mode I loading, in which case $G = (1-\nu)K_I^2/2\mu$, the above criterion reduces to

$$G = 8\frac{1+(1-\nu)\tan^2\phi}{(1+\cos\theta)\sin^2\theta}\gamma_{us} \tag{51}$$

for dislocation nucleation, which may be compared to

$$G = 2\gamma_s \tag{52}$$

(γ_s = surface energy) for Griffith cleavage. Hence, crack tip blunting by dislocation nucleation should occur before conditions for Griffith cleavage decohesion are met if the latter G exceeds the former, which happens for the isotropic solid when

$$\frac{\gamma_s}{\gamma_{us}} > 4\frac{1+(1-\nu)\tan^2\phi}{(1+\cos\theta)\sin^2\theta}. \tag{53}$$

Cleavage occurs before the tip can blunt when the inequality is reversed. The critical γ_s/γ_{us} ratio is, however, usually quite sensitive to deviations from pure mode I loading. For example, if x and z denote fractional shear loadings, defined by writing $K_{II} = xK_I$ and $K_{III} = zK_I$, then the inequality to be met for emission before cleavage is

$$\frac{\gamma_s}{\gamma_{us}} > \frac{4[1+x^2+z^2/(1-\nu)][1+(1-\nu)\tan^2\phi]}{(1+\cos\theta)[\sin\theta+(3\cos\theta-1)x+2z\tan\phi]^2}. \tag{54}$$

Consider a case of interest for bcc solids: a crack on a {100} plane with tip along a ⟨100⟩-type direction, so as to intersect a {110} slip plane on which ⟨111⟩ slip can occur. In that case, $\theta = 45^\circ$ and $\phi = \arctan(1/\sqrt{2}) = 35.3^\circ$. Thus, for pure mode I loading we require $\gamma_s/\gamma_{us} > 6.3$ for dislocation nucleation to occur before Griffith cleavage, but the required ratio reduces nearly by a half, to $\gamma_s/\gamma_{us} = 3.5$ (if $\nu = 0.3$), when K_{II} and K_{III} are just 10% of K_I (i.e. $x = z = 0.1$). Implications for specific solids are discussed later, after reviewing some estimates of γ_{us}.

For the nucleation of dissociated dislocations with $\theta \neq 0$, a geometry of interest for fcc solids is considered, with a crack on a {100} plane and tip along a ⟨110⟩ direction, and it is assumed that the most stressed {111} slip plane is that at $\theta = 54.73^\circ$, and that the loading is such that the first partial to nucleate involves slip along the ⟨211⟩ direction at $\phi_A = 0^\circ$ with the second at $\phi_B = 60^\circ$. Then K_A and K_B of the earlier discussion of dissociated dislocations can be replaced by K_A^{eff} and K_B^{eff}, defined like K_A and K_B in (34) but in terms of K_{II}^{eff} and K_{III}^{eff}. For the special θ and ϕs considered, these quantities are

$$K_A^{\text{eff}} = 0.363(K_I + 0.897K_{II}), \quad K_B^{\text{eff}} = 0.769K_{III} + 0.5K_A^{\text{eff}}. \tag{55}$$

It is assumed that $K_{II} \geqslant 0$ and $K_{III} \geqslant 0$. If not, the same phenomena will occur relative to $\theta = -54.73^\circ$ if $K_{II} < 0$ and to $\phi_B = -60^\circ$ if $K_{III} < 0$, so K_{II} and K_{III} can here be interpreted as $|K_{II}|$ and $|K_{III}|$.

Reading from the earlier results, interpreted approximately in terms of the effective shear stress intensity factors, the 0° partial will indeed be the first to nucleate when $K_{III} < 0.179(K_I + 0.897K_{II})$, and the nucleation condition [from (35)] for that first partial is

$$K_I + 0.897K_{II} = 2.75\sqrt{2\mu\gamma_{us}/(1-\nu)}. \tag{56}$$

This is shown as the dashed line in Fig. 8, which is analogous to the mixed-mode

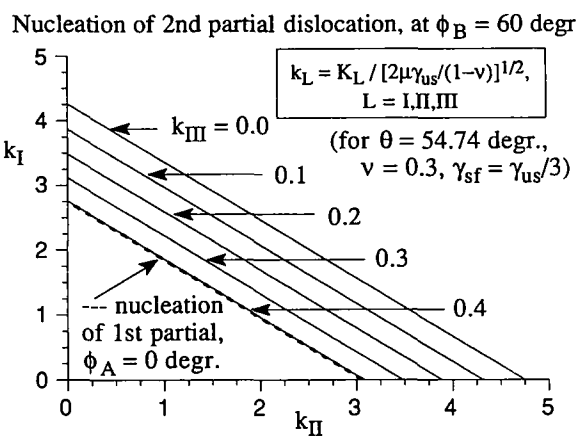

FIG. 8. Combinations of K_I, K_{II} and K_{III} for nucleation of the second of two partial dislocations in a fcc crystal with crack on {100} plane, with tip along ⟨110⟩ direction so that the relevant {111} slip plane is at $\theta = 54.74^\circ$; the first partial is assumed to nucleate with $\phi = 0^\circ$ and the second with $\phi = 60^\circ$.

nucleation diagrams of LIN and THOMSON (1986). The nucleation condition for the second partial, at $\phi_B = 60°$, is then, from (39), (41), (42) and (55),

$$0.769K_{III}+0.5\sqrt{[0.363(K_I+0.897K_{II})]^2-\frac{2\mu}{1-\nu}\gamma_{sf}}$$

$$=\sqrt{\frac{(4-3\nu)\mu}{2(1-\nu)}(\gamma_{us}-\gamma_{sf})}. \tag{57}$$

For pure mode I loading, this is

$$K_I = 2.75\sqrt{2\mu[(4-3\nu)\gamma_{us}-3(1-\nu)\gamma_{sf}]/(1-\nu)}, \tag{58}$$

or $K_I = 4.26\sqrt{2\mu\gamma_{us}/(1-\nu)}$ when $\nu = 0.3$ and $\gamma_{sf} = \gamma_{us}/3$. The combined loading result is plotted in Fig. 8, based on $\nu = 0.3$ and $\gamma_{sf} = \gamma_{us}/3$, for various values of K_{III}. The nucleation condition is extremely sensitive to K_{III}: while the numerical factor 2.75 in (56) above increases to 4.26 for nucleation of the second partial when $K_{III} = 0$, that factor is reduced back to 2.75 (so that there is spontaneous nucleation of the second partial) when K_{III} is increased so that an analogously defined numerical factor for K_{III} reaches only 0.404.

From (56) and (52), the first partial will nucleate before the Griffith cleavage condition is met, under pure mode I loading of the fcc configuration considered, if $\gamma_s/\gamma_{us} > 3.8$. Since $\phi_A = 0$, this result is insensitive to mode III loading, at least as long as $|K_{III}| < 0.179K_I$, so that the $\phi = 0°$ partial is actually the first to nucleate. If there is also a 10% mode II loading ($x = 0.1$), the inequality changes somewhat, to $\gamma_s/\gamma_{us} > 3.2$.

Under pure mode I loading, the second partial, and hence the complete fcc dislocation, nucleates before Griffith cleavage if, from (58) and (52),

$$\gamma_s/\gamma_{us} > 3.8[4-3\nu-3(1-\nu)\gamma_{sf}/\gamma_{us}], \tag{59}$$

which is $\gamma_s/\gamma_{us} > 9.1$ when $\nu = 0.3$ and $\gamma_{sf} = \gamma_{us}/3$. However, as anticipated from the discussion above, this result is extremely sensitive to small shear mode contributions, especially in mode III. Thus, for loading with K_{II} and K_{III}, both 10% of K_I, and with $\nu = 0.3$ and $\gamma_{sf} = \gamma_{us}/3$, the inequality becomes $\gamma_s/\gamma_{us} > 4.2$, so that there is a reduction to less than a half of the γ_s/γ_{us} value required for nucleation prior to cleavage under pure mode I loading.

Because of the strong sensitivity to shear loadings illustrated here, and in the earlier bcc discussion, it should rather commonly be the case that dislocations emerge from (nominally) tensile loaded cracks in solids which violate the γ_s/γ_{us} requirement for ductility under pure tensile loading by as much as, say, a factor of 2.

7. Comparison with Nucleation Model Based on Full Dislocation and Core Cut-off

In general, previous treatments of dislocation nucleation (RICE and THOMSON, 1974; LIN and THOMSON, 1986; ANDERSON, 1986) have modeled a pre-instability dislocation feature at the crack tip as a fully formed dislocation in the configuration

either of a line lying parallel to the crack tip and displaced a distance r from it, or of a localized dislocation loop emerging from the crack tip. The line model is easier to treat and can be compared directly to the result of the previous section. The net configurational force P on such a dislocation is the sum of that due to the applied loading plus the image-like effect caused by the traction-free crack faces nearby (RICE and THOMSON, 1974):

$$P = \{[K_I f_I(\theta) + K_{II} f_{II}(\theta)]\cos\phi + K_{III} f_{III}(\theta)\sin\phi\} b/\sqrt{2\pi r} - \mu b^2[\cos^2\phi + (1-\nu)\sin^2\phi]/4\pi(1-\nu)r. \quad (60)$$

A nucleation condition has traditionally been extracted from this expression by assuming that nucleation will occur if $P > 0$ whenever $r > r_o$ (= core cut-off). That gives, as the threshold for nucleation (i.e. making $P = 0$ when $r = r_o$),

$$[K_I f_I(\theta) + K_{II} f_{II}(\theta)]\cos\phi + K_{III} f_{III}(\theta)\sin\phi = \mu b[\cos^2\phi + (1-\nu)\sin^2\phi]/2(1-\nu)\sqrt{2\pi r_o}. \quad (61)$$

If r_o is chosen in a certain way, this can be made to coincide with the more exact result (50) of the previous section. Thus, for dislocations of respective edge and screw character relative to the crack, the choice of r_o would be

$$(r_o)_{\text{edge}} = \mu b^2/16\pi(1-\nu)\gamma_{us}, \quad (r_o)_{\text{screw}} = \mu b^2/16\pi\gamma_{us}. \quad (62)$$

Estimates of γ_{us} discussed later for metals range from approximately $0.025\mu b$ to $0.10\mu b$. Thus, with $\nu = 0.3$, the fully-formed line dislocation model gives results in agreement with those derived more convincingly here, based on the Peierls concept, if the core cut-off radius $r_o \approx 0.28$–$1.14b$ for edge dislocations and $r_o \approx 0.20$–$0.80b$ for screw dislocations.

8. Width of the Incipient Dislocation Zone at Instability

The width of the incipient dislocation zone at the moment of instability is also of interest. It will be seen that the width at a crack tip is, at the moment of instability, a moderately broad feature compared to a lattice spacing, thus making more appropriate the use of the Peierls concept. Indeed, PEIERLS (1940) laments towards the end of his paper that the dislocation core size which he calculated, for an isolated dislocation in an otherwise perfect lattice, was sufficiently narrow compared to b that the concept of a continuously distributed core displacement, amenable to analysis by continuum elasticity, becomes problematical. The results for nucletion at a crack tip appear to be more favorable.

The core width at nucleation instability cannot be obtained exactly from our present considerations and requires a full numerical solution of (9). Some such results have been obtained by BELTZ and RICE (1991a) based on a $\tau = f(\delta)$ relation obtained from the Frenkel sinusoid. However, an elementary estimate of the width of the core region can be made in the following inverse manner: since the $\tau = f(\delta)$ relation rises from $\delta = 0$ with an initially vertical tangent, matters are simplified by considering model

relations $f(\delta)$ for which $\delta = 0$ up to a finite value of τ. In that case the zone of the incipient dislocation, with $\delta > 0$, will be limited to some finite distance R, to be estimated, ahead of the crack tip. If $\tau(x_1)$ denotes the spatial distribution of stress over $0 < x_1 < R$, then by using an elementary elastic solution for semi-infinite cracks [e.g. RICE (1968b)] one may see that for pure mode II loading of an incipient edge configuration with $\theta = 0$ (like for Fig. 3), the distribution of δ on $x_1 < R$ is given by

$$\frac{\mu}{2(1-\nu)}\frac{\mathrm{d}\delta(x_1)}{\mathrm{d}x_1} = -\frac{K_{II}}{\sqrt{2\pi(R-x_1)}} + \frac{1}{\pi}\int_0^R \frac{\tau(t)}{x_1-t}\sqrt{\frac{R-t}{R-x_1}}\,\mathrm{d}t \tag{63}$$

whereas the distribution of stress $\sigma_{12}(x_1, 0)$ $(=\tau)$ along $x_1 > R$ is given by

$$\sigma_{21}(x,0) = \frac{K_{II}}{\sqrt{2\pi(x_1-R)}} - \frac{1}{\pi}\int_0^R \frac{\tau(t)}{x_1-t}\sqrt{\frac{R-t}{x_1-R}}\,\mathrm{d}t. \tag{64}$$

The idea, now, is to assume a distribution of τ with x_1, vanishing at $x_1 = 0$ [so as to correspond to maximum $\Phi(\delta)$ there, and thus to be consistent with the crack tip configuration at nucleation instability]. R is related to K_{II} so as to cancel any singularity at $x_1 = R$, and then a distribution $\delta(x_1)$ is calculated, constraining parameters of the model so that $\delta(0) = b/2$. This procedure will define a τ vs δ relation and, if the relation looks not too unreasonable, the procedure may be accepted as giving an approximate solution.

To keep things simple, a distribution of τ with x_1 in the form of a parabola can be assumed, vanishing at $x_1 = 0$:

$$\tau = (3\tau_{max}/4)(x_1/R)(4-3x_1/R), \tag{65}$$

where τ_{max} is the maximum value of τ, attained at $x_1 = 2R/3$, whereas the value of τ at $x_1 = R$ is $3\tau_{max}/4$. The factors of 4 and 3 are chosen for aesthetic reasons, as they may be shown to define the unique parabola for which the present procedure gives a distribution of σ_{21} $(=\tau)$ which is not only continuous but has a continuous slope at $x_1 = R$. To cancel the singularity,

$$R = 25\pi K_{II}^2/128\tau_{max}^2 = 25\pi\gamma_{us}\mu/64(1-\nu)\tau_{max}^2, \tag{66}$$

where the J-integral analysis ensures that γ_{us} here will be consistent with the $\tau = f(\delta)$ relation implied by the analysis. The integrals above then show that

$$\frac{\mu}{2(1-\nu)}\frac{\mathrm{d}\delta(x_1)}{\mathrm{d}x_1} = -\frac{3\tau_{max}}{2\pi}\left[\frac{1}{2}(1+2\xi-3\xi^2)\ln\left(\frac{1+\sqrt{\xi}}{|1-\sqrt{\xi}|}\right)+(3\xi-1)\sqrt{\xi}\right] \tag{67}$$

on $x_1 < R$, where $\xi = (R-x_1)/R$, and that

$$\sigma_{21}(x_1,0) = \frac{3\tau_{max}}{2\pi}[(1-2\eta-3\eta^2)\tan^{-1}(1/\sqrt{\eta})+(3\eta+1)\sqrt{\eta}] \tag{68}$$

on $x_1 > R$, where $\eta = (x_1-R)/R$.

Demanding now that $b/2$ be the integral of $-\mathrm{d}\delta/\mathrm{d}x_1$ from $x_1 = 0$ to $x_1 = R$,

$$b/2 = 2.5465(1-\nu)\tau_{max}R/\mu \tag{69}$$

is obtained which, when combined with the expression for R above, shows that

$$\gamma_{us} = \tau_{max}b/3.125 \tag{70}$$

is a feature of the $\tau = f(\delta)$ relation implied by the assumed parabolic stress distribution. The relation itself, having threshold $0.75\tau_{max}$, is plotted in Fig. 9(a), as obtained by cross plotting τ and δ from the above equations along $0 < x_1 < R$, and has, perhaps, a not too unreasonable shape. The numerical factor of 3.125 in (70) compares well to π, which is the similar factor based on $\tau = f(\delta)$ from the Frenkel sinusoid. Figure 9(b) shows the resulting spatial variations of τ and δ, and the above elimination of τ_{max} shows that the distance R is given by

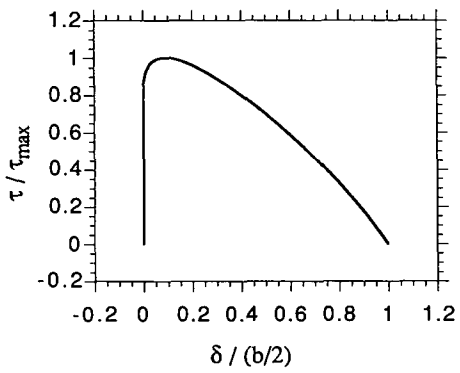

(a)

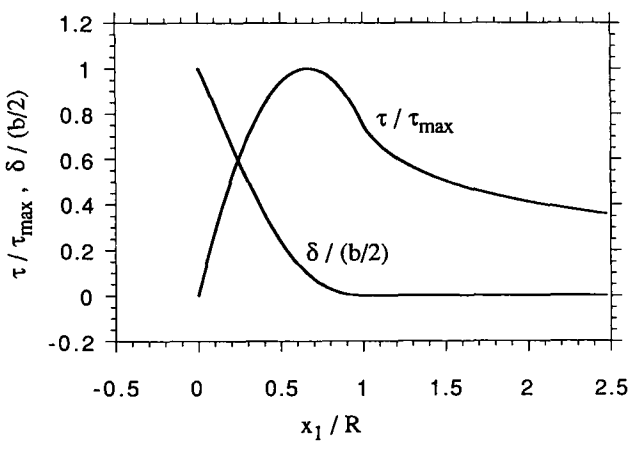

(b)

FIG. 9. (a) Form of the τ vs δ relation, and (b) distribution of τ and δ at nucleation instability, implied by a parabolic variation of τ with x_1 over distance R, estimated (see text) to typically be of order 2–7b.

$$R = 0.1257\mu b^2/(1-\nu)\gamma_{us}. \tag{71}$$

Since (next section) representative estimates of γ_{us} for metals run from about $0.025\mu b$ to $0.10\mu b$, this gives (with $\nu = 0.3$) $R \approx 2$–$7b$, a substantial size.

If γ_{us} in the above expression for R is estimated from the Frenkel sinusoid, then $\gamma_{us} = \mu b^2/2\pi^2 h$ and $R = 2.48h/(1-\nu)$. This may be compared with Peierls' width, also based on the Frenkel form, of $h/2(1-\nu)$ (HIRTH and LOTHE, 1968) for an isolated dislocation. This width is the distance over which τ diminishes from its peak value to its unstable zero value at $\delta = \Delta = b/2$. The corresponding width is $2R/3$ for the crack tip model discussed above, and $2R/3 = 1.65h/(1-\nu)$, which is 3.3 times the width for Peierls' isolated dislocation. This shows the core broadening in an elementary way. The numerical solution of BELTZ and RICE (1991a), based on the Frenkel sinusoid with $h = b$ and with $\nu = 0.3$, gives a similar result with the numerical factor estimated here as 3.3 being about 2.8 instead.

NABARRO (1947) solved the problem corresponding to that of Peierls for the case of two coplanar dislocations of opposite sign, attracting one another and subjected to a stress just sufficing to hold them in unstable equilibrium, in an otherwise perfect lattice. This is a nice analog of the problem of dislocation nucleation from a crack tip, particularly when it is recalled that RICE and THOMSON (1974) show that the self force on a line dislocation at distance r from a crack tip is the attractive force caused by an oppositely signed dislocation lying at distance $2r$ away in an uncracked, otherwise perfect solid [e.g. (60)]. Like what is inferred here, NABARRO's (1947) results show that the core widens considerably from the Peierls size as the two dislocations are brought close to one another.

9. ESTIMATES OF THE UNSTABLE STACKING ENERGY, γ_{us}

Frenkel estimates. The simplest estimate of γ_{us} is based on the Frenkel sinusoid. This is rewritten here, for shear relative to atomic planes spaced by h, as

$$\tau = (\mu_{\text{slip}} b_{\text{eff}}/2\pi h) \sin (2\pi\Delta/b_{\text{eff}}) \tag{72}$$

to emphasize that the modulus, μ_{slip}, should be that for shear relative to the slip system, and given as $\mu_{\text{slip}} = (c_{11}-c_{12}+c_{44})/3$ for the fcc and bcc crystal slip systems considered here. Also the Burgers vector is replaced by an effective value, b_{eff}, to emphasize that in some cases the Δ ($= b_{\text{eff}}/2$) at maximum energy γ_{us}, i.e. at the unstable zero of τ, may not coincide with $b/2$. Thus

$$\gamma_{us(\text{Frenkel})} = \mu_{\text{slip}} b_{\text{eff}}^2/2\pi^2 h. \tag{73}$$

This result is shown in the dimensionless form $\gamma_{us(\text{Frenkel})}/\mu_{\text{slip}} b$ as the first numerical column of Table 1 for partial dislocation on {111} planes in fcc solids and for complete dislocation on two common slip planes, {110} and {211}, in bcc solids. For the fcc and first bcc case $b_{\text{eff}} = b$ (where, consistently with earlier use, in the fcc case b corresponds to that of a Shockley partial). However, the Frenkel model is expected to give a poor representation of the $\tau = F(\Delta)$ relation for shear on the {211} plane in the bcc case (VITEK *et al.*, 1972), especially for shear in the twinning direction on that

TABLE 1. *Estimates of* $\gamma_{us}/\mu_{slip}b$†

Solid	Frenkel sinusoid ($b_{eff}^2/2\pi^2bh$)	Embedded-atom models, block-like shear	Density functional, homogeneous simple shear strain ($W_{max}h/\mu_{slip}b$)
(1) fcc, partial dislocations, $\langle 211\rangle\{111\}$, $b = a_0/\sqrt{6}$, $h = a_0/\sqrt{3}$, $b_{eff} = b$:			
Al	0.036	0.026(u)	0.042(r), 0.043(u)
Cu	0.036	—	0.042(u)
Ir	0.036	—	0.034(r), 0.043(u)
Ni	0.036	0.026(u)	—
(2) bcc, $\langle 111\rangle\{110\}$, $b = \sqrt{3}a_0/2$, $h = a_0/\sqrt{2}$, $b_{eff} = b$:			
Fe	0.062	0.038(r), 0.045(u)	—
(3) bcc, $\langle 111\rangle\{211\}$, $b = \sqrt{3}a_0/2$, $h = a_0/\sqrt{6}$, $b_{eff} = 2b/3$–b:			
Cr	0.048–0.108	—	0.069(u)
Mo	0.048–0.108	—	0.056(u)
Nb	0.048–0.108	—	0.093(u)
V	0.048–0.108	—	0.100(u)
W	0.048–0.108	—	0.060(u)

†r = relaxed in direction normal to slip plane; u = unrelaxed.

plane, in which direction it is possible that slip energy Φ (or Ψ) has a local maximum corresponding to the twinned structure, as it climbs towards γ_{us}. The geometry of shear in the anti-twinning direction (PAXTON *et al.*, 1991) seems somewhat simpler and the Frenkel model might apply approximately with the Δ at γ_{us} reduced from $b/2$ to a value perhaps as low as $b/3$. Thus, for that case, b_{eff} is given a range $2b/3$–b in Table 1, resulting in the $\gamma_{us(Frenkel)}$ range shown.

To go beyond these simple estimates requires models of atomic potentials in solids. In principle, the energy γ_{us} could be determined by a quantum mechanical computation, based on (electron) density functional theory in the local density approximation, of the ground state energy of the configuration for which one half of a lattice is rigidly shifted relative to the other along a slip plane, so as to coincide with the unstable stacking [like in configuration (d) in Fig. 2]. The analysis of such atomic geometries seems consistent with the present level of development of density functional computations, and is to be encouraged in the future.

For the present it is necessary to be content with empirical atomic models. A recently developed class of these, going beyond pair potentials and thus avoiding Cauchy symmetry of crystal moduli, have been formulated within the *embedded-atom method* (DAW and BASKES, 1984) and have found extensive applications to solid state phenomena, including interfacial structure and deformation and fracture. A few results for γ_{us} based on such models are now summarized.

Embedded-atom models. Such embedded-atom models as have been introduced seem to lead to lower estimates of γ_{us} than does the Frenkel model. The results will be different for direct shear with no relaxation in the direction normal to the slip plane (the most commonly available case), and for relaxed shear for which the lattice spacing h is allowed to dilate during shear so as to keep zero normal stress.

CHEUNG (1990) [see also CHEUNG *et al.* (1991)] employed an embedded-atom model for bcc Fe and, from plots of his potential for $\{110\}\langle 111\rangle$ shear, it may be inferred that $\gamma_{us(EAM)} = 0.43$ (relaxed) to 0.52 (unrelaxed) J/m^2. The dimensionless $\gamma_{us(EAM)}/\mu_{slip}b$ is entered for Fe in the second numerical column of Table 1 where, here and next, μ_{slip} is the slip system shear modulus that is consistent with the embedded-atom potentials used.

SUN *et al.* (1991b) and Sun (private communication, 1991) have done similar calculations based on embedded-atom models for $\{111\}\langle 211\rangle$ shears forming partial dislocation in fcc metals. These are for the respective cases of Al modeled by the potentials of HOAGLAND *et al.* (1990) and FOILES and DAW (1987), and Ni by potentials of FOILES *et al.* (1986). These results, both unrelaxed, are $\gamma_{us(EAM)} = 0.092$ J/m^2 for Al and 0.260 J/m^2 for Ni; both numbers correspond to nearly the same $\gamma_{us(EAM)}/\mu_{slip}b$, of 0.026 as entered in Table 1. Relaxed $\gamma_{us(EAM)}$ values are not presently available for Al and Ni.

It may be noted that the unrelaxed values of $\gamma_{us(EAM)}/\mu_{slip}b$ cited for Fe, Ni and Al are all of the order of 72–73% of the corresponding $\gamma_{us(Frenkel)}/\mu_{slip}b$. Thus, for later purposes (Table 2) in dealing with $\{111\}$ plane partial dislocations in a large class of fcc solids and with $\{110\}$ plane dislocations in a large class of bcc solids, for most of which embedded atom model results for γ_{us} are not available, the rough estimate $\gamma_{us(EAM)} = 0.7\gamma_{us(Frenkel)}$ is tentatively used in all cases.

Density functional theory. No directly relevant calculation for the block-like shear of one part of a metal crystal relative to another seems yet to have been reported based on quantum mechanics via density functional theory. However, such calculations appear to be feasible, as DUESBERY *et al.* (1991) have reported energy surfaces for shear of Si along $\{111\}$ planes in a manner corresponding to the introduction of an intrinsic stacking fault. The DUESBERY *et al.* (1991) work also shows that empirical potentials, as available for Si, may agree reasonably with the quantum mechanical calculations for one direction of shear but poorly for another direction on the same crystal plane.

PAXTON *et al.* (1991) used density functional theory in the local approximation to analyze stress–strain relations of homogeneously strained crystals, in fcc cases corresponding to simple shear parallel to $\{111\}$ planes in $\langle 211\rangle$-type directions, and for bcc cases to simple shear parallel to $\{211\}$ planes in $\langle 111\rangle$-type directions. These are shears leading to twinning transformations (in the softer direction of shear in each case). Paxton *et al.* report the maximum stress and also the maximum strain energy (say, W_{max}, on a unit volume basis) encountered for simple shear in the twinning direction and in the opposite, or anti-twinning direction. The strain energy maximum, W_{max}, is a rough analog of γ_{us}. Both correspond to maximum energies along a shear path, but for block-like shear of one half the lattice relative to the other in the case of γ_{us} [like in Fig. 2, illustration (d)], and for homogeneous simple shear strain of the entire lattice in the case of W_{max}.

A quantity somewhat like γ_{us} may be formed from W_{max} in the following way: since W_{max} is the maximum energy per unit volume in simple shear strain, $W_{max}h$ is the maximum energy per unit area of slip plane associated with an interplaner separation h. This might be considered comparable to γ_{us} and thus the final column in Table 2 shows $W_{max}h/\mu_{slip}b$ based on W_{max} from PAXTON *et al.* (1991) and using experimental

μ_{slip} values [expected to correspond within about 10% of those estimated from the density functional calculations (Paxton, private communication, 1991)]; W_{max} for the twinning sense is used for the fcc partial dislocation comparisons, and in the anti-twinning sense, suggested in PAXTON *et al.* (1991), for complete {211} bcc dislocation comparisons. It is interesting that these values seem approximately compatible with the Frenkel estimates.

The experimental values for μ_{slip} used in the last column of Table 1 (and in Table 2) are from HIRTH and LOTHE (1968) and, if not there, from BRANDES (1983) or ANDERSON (1986). Lattice parameters a_o, used to get b, are from ASHCROFT and MERMIN (1976).

10. DUCTILE VS BRITTLE CRACK TIP RESPONSE

In using the results of this paper to discuss ductile vs brittle response, in the sense of asking whether conditions for dislocation nucleation will or will not be met prior to Griffith cleavage, it is well to keep the following factors in mind.

(a) Dislocation nucleation is a process susceptible to thermal activation. The analysis given here is, essentially, of temperature $T = 0$ response. The critical Ks for nucleation will be reduced somewhat at finite T. The Peierls concept gives a route to treat thermally activated nucleation and some related concepts have already been uncovered in the J-integral analysis of the crack tip shear (Fig. 4, point C) in the 2D saddle point configuration of $\delta(r)$. The fuller evaluation of the activation energy for dislocation nucleation is beyond the scope of the present work and a followup paper is planned on it. While the K level for dislocation nucleation in some finite waiting time can, in principle, be reduced arbitrarily by an increase in T (some solids may melt before there is any substantial reduction), it is interesting that the K for cleavage cannot be reduced arbitrarily and always has the Griffith level (at that T) as a lower bound. Thus an increase in T should generally ease dislocation nucleation more than cleavage, and favor ductility. The considerations in the rest of this section are for low T, when thermal activation is not an important factor.

(b) The present analysis of dislocation nucleation is approximate in many respects, and thus it will be difficult to draw definitive conclusions on ductile vs brittle response in the several borderline cases that will be seen to arise. Elastic anisotropy has not been accounted for in the nucleation criteria presented, the treatment of $\theta \neq 0$ is approximate based on the K^{eff} idea, and effects of normal stresses on dislocation-forming shear motions have not been considered [along with other possible limitations of the constrained-path procedure (Section 4)]. Most importantly, perhaps, we have no very reliable estimates of γ_{us}; the $\gamma_{us(\text{Frenkel})}$ and $\gamma_{us(\text{EAM})}$ values of Table 1 may contain large errors. Also, reliable values of γ_{sf}, needed in the fcc cases, are not available for most solids.

(c) Dislocation processes not directly associated with nucleation from a crack tip may actually control brittle vs ductile response in many cases. For example, in soft solids with a high density of mobile dislocation, it may never be possible to build up enough stress at a crack tip to meet either a Griffith cleavage or a dislocation nucleation criterion, so the issue of which requires the greater local K value becomes irrelevant.

Also, in solids for which dislocation mobility is low, easy nucleation of dislocations from a crack tip does not necessarily imply relaxation of stresses; cleavage may occur because such dislocations cannot move readily enough away from the crack tip so as to relax stress in its vicinity.

Accepting these limitations, consider Table 2. Estimates of the surface energy γ_s at $T = 0$, based on measurements that have been extrapolated to low temperature or, where noted by the cross, on correlations thus established with formation energies, are shown in the first column based on TYSON (1975). Shear moduli μ_{slip} and b are also shown (b is for a Shockley partial dislocation in the fcc and diamond cubic cases, and for a complete dislocation in the bcc cases), and the Frenkel estimate $\gamma_{us(Frenkel)} = \mu_{slip}b^2/2\pi^2h$ is calculated from them, as $0.036\mu_{slip}b$ for partial dislocations in fcc and rather uncertainly diamond cubic, and $0.062\mu_{slip}b$ for complete dislocations on the $\{110\}$ plane in bcc.

We can therefore calculate the ratios of γ_s/γ_{us} shown in the last two columns of Table 2, based, respectively, on $\gamma_{us(Frenkel)}$ and $\gamma_{us(EAM)}$, with the latter approximated as $0.7\gamma_{us(Frenkel)}$.

TABLE 2. *Material properties and* γ_s/γ_{us} *ratios*

Solid	γ_s ($T = 0$) (J/m^2)	μ_{slip} (GPa)	b (nm)	$\gamma_{us(Frenkel)}$ (J/m^2)	$\gamma_s/\gamma_{us(Frenkel)}$	$\gamma_s/\gamma_{us(EAM)}$
fcc metals:						
Ag	1.34	25.6	0.166	0.15	8.8	12.5
Al	1.20	25.1	0.165	0.15	8.1	11.5
Au	1.56	23.7	0.166	0.14	11.0	15.7
Cu	1.79	40.8	0.147	0.22	8.3	11.8
Ir	2.95†	198	0.156	1.1	2.7	3.8
Ni	2.27	74.6	0.144	0.39	5.9	8.4
Pb	0.61	7.27	0.201	0.053	11.6	16.6
Pt	2.59	57.5	0.160	0.33	7.8	11.2
bcc metals:						
Cr	2.32	131	0.250	2.0	1.1	1.6
Fe	2.37	69.3	0.248	1.1	2.2	3.2
K	0.13†	1.15	0.453	0.032	4.0	5.7
Li	0.53†	3.90	0.302	0.073	7.3	10.4
Mo	2.28	131	0.273	2.2	1.0	1.5
Na	024†	2.43	0.366	0.055	4.4	6.2
Nb	2.57	46.9	0.286	0.83	3.1	4.4
Ta	2.90	62.8	0.286	1.1	2.6	3.7
V	2.28†	50.5	0.262	0.82	2.8	4.0
W	3.07	160	0.274	2.7	1.1	1.6
Diamond cubic:						
C	5.79†	509	0.145	2.7	2.2	3.1
Ge	1.20†	49.2	0.231	0.41	2.9	4.2
Si	1.56†	60.5	0.195	0.42	3.7	5.2

†γ_s based on correlation with formation energy (TYSON, 1975). $\mu_{slip} = (c_{11}-c_{12}+c_{44})/3$. $b = b_{partial} = a_0\langle 211\rangle/6$ for fcc and diamond cubic; $b = a_0\langle 111\rangle/2$ for bcc. $\gamma_{us(Frenkel)} = 0.036\mu_{slip}b$ for fcc and diamond cubic; $\gamma_{us(Frenkel)} = 0.062\mu_{slip}b$ for bcc. $\gamma_{us(EAM)}$ equated to $0.7\gamma_{us(Frenkel)}$.

To recall now the conclusions drawn in Section 6, it was shown that the dislocation nucleation condition is met before that for Griffith cleavage, for the {100} cracks considered, if, under pure mode I loading,

$$\gamma_s/\gamma_{us} > 9.1 \text{ (fcc) or } 6.3 \text{ (bcc)}. \tag{74}$$

Both required ratios were strongly reduced by small deviations from pure mode I, the fcc case most. For example, with shear mode stress intensity factors set at 10% of K_I, the requirements for dislocation nucleation to occur before Griffith cleavage dropped to

$$\gamma_s/\gamma_{us} > 4.2 \text{ (fcc) or } 3.5 \text{ (bcc)}. \tag{75}$$

(The fcc numbers in each case also depend on γ_{sf}/γ_{us}, which has been taken as 1/3 in the above inequalities; $\nu = 0.3$ is used there too.)

If the $\gamma_{us(\text{EAM})}$ estimates are tentatively accepted as being close to correct, thus using the last column in Table 2 as estimates of γ_s/γ_{us}, the following conclusions are arrived at for the fcc metals: all the fcc metals except Ni and Ir are incapable of cleaving. If the small disparity between 9.1 and the 8.4 ratio shown for Ni is real, and not just an artifact of the approximations made, then Ni should be cleavable under pure mode I loading. Still, a very small amount of loading in the two shear modes (of order 2% of K_I) suffices to cause ductile response. Ir would still cleave even with a 10% shear mode loading but would behave in a ductile manner with slightly greater shear present. This is consistent with the known cleavage of Ir. If the conclusions on Ni being cleavable under pure mode I are supported after accounting for some of the approximations of the present treatment noted in (b) above, then it may be fruitful to attempt careful mode I loading tests on Ni crystals at low T to look for cleavage. As an indication that Ni may, plausibly, be thought of as a borderline material, in a brittle vs ductile sense, it is interesting to note that grain boundaries in Ni are rather easily rendered cleavable by segregation of S there and by the presence of H.

If the true γ_{us} is close to the Frenkel estimate then, according to Table 2, even Pt, Al, Cu and Ag should be borderline cleavable at low T if loaded in perfect mode I, at least if consideration of elastic anisotropy and other factors of (b) above do not change things. However, a little loading in the two shear modes, less than 1% of K_I for Ag, 2% for Cu and Al, and 3% for Pt, shifts the balance in favor of dislocation nucleation.

This simplified discussion of fcc solids has assumed the same $\gamma_{us}/\mu_{\text{slip}}b$ in all materials and also the same γ_{sf}/γ_{us}.

For the bcc metals, again first assume the $\gamma_{us(\text{EAM})}$ is close to correct so that the last column of Table 2 gives γ_s/γ_{us}. Then the alkali metals, Li, Na and K, are the standouts in terms of ductility. The γ_s/γ_{us} for Li is well above the margin of 6.3 for pure mode I, and Na is so near that a lot less than 1% loading in the shear modes (or perhaps a T only moderately above 0) would favor dislocation nucleation over Griffith cleavage in it, and about 2% shear modes loading would suffice for K. This is consistent with the general malleability of the alkali metals.

The vanadium subgroup of the transition metals, in the order Nb, V and Ta, also stand out in Table 2. They fall below the threshold for the ductile crack tip response for pure mode I loading, but fit comfortably within the border for ductile response

when mode I is accompanied by 10% loadings in the shear modes. Fe is predicted to be clearly cleavable, although it should be ductilized by 12% or so shear loadings. Fe may also be a case for which there is relatively strong sensitivity of the effective γ_{us} to normal stress, as suggested by the relaxed–unrelaxed difference for it in Table 1 and by CHEUNG *et al.* (1991); that would favor more ductile response. By comparison, the chromium subgroup of transition metals, Cr, Mo and W, seem by our criterion to be irredeemably brittle.

If the Frenkel estimates of γ_{us} are, instead, somewhat closer to the mark, then the results of Table 2 still suggest that Li cannot be cleaved. The other alkali metals are less borderline, but fit well within the 10% shear mode margin, whereas the vanadium subgroup would require about 11–14% shear for ductilization, and Fe around 15%.

Diamond cubic non-metals are also shown in Table 2 and γ_{us} has been listed for them as for fcc metals, assuming that dislocations are generated by a partial route on {111} planes. All of the diamond cubic solids are predicted to be cleavable by these considerations. It is interesting, however, that Si and Ge rate higher than Ir which, while known to cleave, can nevertheless show substantial dislocation elasticity. Thus, while the γ_s/γ_{us} ratios suggest that Si should show dislocation nucleation from a crack tip at low temperatures if shear mode loadings of the order 10% of K_I are present, the low mobility of any such dislocations, once nucleated, may condemn Si even then to a brittle response. It will be interesting to see what the relatively high γ_s/γ_{us} for Si, among the cleavable fcc and diamond cubic solids, implies for nucleation eased by thermal activation at higher T.

Since the rough γ_{us} estimates used in Table 2 scale directly with $\mu_{\text{slip}}b$ for a given crystal class, the characterization of a crack tip response as brittle or ductile on the basis of the size of γ_s/γ_{us} shown in Table 2 is equivalent to characterization on the basis of $\gamma_s/\mu_{\text{slip}}b$, much as advocated by ARMSTRONG (1966) and RICE and THOMSON (1974).

11. SUMMARY AND CONCLUSIONS

A new analysis of dislocation nucleation from a crack tip is presented based on the Peierls concept as applied to a slip plane emanating from the tip. Shear stress along the slip plane is a periodic function of the amount of slip. An exact solution for the nucleation criterion is found when the crack and slip plane coincide, at least within the simplifying assumption that shear sliding between lattice planes, in forming a dislocation, is negligibly affected by normal stress. The exact solution is also extended to the nucleation of dissociated dislocations, with complete results found for the nucleation of a pair of Shockley partials in fcc solids. For cases of greater interest, in which the slip and crack planes do not coincide ($\theta \neq 0$) but, rather, intersect along the crack tip, an approximate solution for the nucleation criterion is given based on effective shear stress intensity factors along the slip plane.

The core width of the incipient dislocation at the threshold of instability is estimated to be about 3 times the corresponding width for an isolated dislocation in an otherwise perfect lattice, so that conditions seem favorable for the use of the Peierls concept.

Further, while previous treatments of nucleation have generally been based on elasticity solutions for fully formed dislocations located very near the crack tip, this analysis shows that maximum shear slippage at the tip is, at the moment of instability, only of the order of half that for a fully formed dislocation.

The results identify a new solid state parameter γ_{us}, called the unstable stacking energy, which measures the resistance to dislocation nucleation at a crack tip. Critical stress intensity factors at nucleation scale with $\sqrt{\gamma_{us}}$. Here γ_{us} is the maximum energy, per unit area, encountered in the block-like shear of one half of a crystal relative to the other, along a slip plane in the direction of shear which forms a lattice dislocation. Also, while the concept is not fully developed here, some features of the 2D activated configuration (energy saddle point) have been derived for a crack tip loaded below the level for instantaneous nucleation.

There are, at present, only quite uncertain estimates of γ_{us}. The sheared atomic lattice geometry to which it corresponds is, however, a relatively simple one, periodic in the two directions along the slip plane and involving simple block-like translation of atoms above and below. Thus, it is to be hoped that the parameter may be susceptible to quantum electronic calculation, and such work is encouraged (the same for stacking fault and anti-phase boundary energy terms, which also enter the nucleation criteria for dissociated dislocations).

Allowing for considerable uncertainties in γ_{us}, the evaluation of the competition over whether the condition for Griffith cleavage, or for dislocation generation and blunting, is met first at a crack tip leads to results that seem generally consistent with the known brittle vs ductile response of fcc and bcc metals. The results also suggest that the outcome of this competition is often extremely sensitive to small amounts of mode II and mode III shear loading superposed on a basic mode I tensile loading; the shear loadings promote ductile response.

There is much to improve on the continuum mechanics of the present analysis. Elastic anisotropy will be relatively straightforward to incorporate, especially at the level of the present development, since every step is readily generalized to cases of general rectilinear anisotropy. The accuracy of the treatment of inclined slip planes by the effective shear stress intensity factor concept needs more careful assessment, and this is partly underway [e.g. BELTZ and RICE (1991b)].

The present approach fails when there is more than a single kinematic variable describing relative motion on the slip plane. This occurs when coupling between different displacement modes is strong, so that one must consider the interaction of dislocation shear displacements with opening and/or orthogonal shear displacements along the slip plane. In this case the requisite input to the nucleation formulation includes much more than γ_{us}, and involves a full potential of form $\Phi^*(\delta_1, \delta_2, \delta_3)$ along the slip plane. A numerical solution to a system of coupled non-linear integral equations is then necessary. Some of the simpler cases have been studied (BELTZ and RICE, 1991a, b; SUN *et al.*, 1991a) but a comprehensive understanding of the results, and of the materials and/or situations in which coupling is important, is not yet at hand. Finally, the new analysis of dislocation nucleation given here, like that formulated by RICE and THOMSON (1974), is developed only for cases in which the crack tip lies in a slip plane. It has been noted (ARGON, 1987; DRAGONE and NIX, 1988) that the maximally stressed slip plane is sometimes one which intersects the crack tip

at a single point but does not contain it. There seems to be no simple way of extending the present approach to such cases.

ACKNOWLEDGEMENT

The study was supported by the Office of Naval Research, Mechanics Division, under grant N00014-90-J-1379, and also by a Fairchild Fellowship held at Caltech at the time when the basic ideas of this analysis were first developed in summer 1989. Perspectives gained in related work since then with G. E. Beltz, I.-H. Lin, Y. Sun and L. Truskinovsky, on further developing the approach to dislocation nucleation outlined here, have added to this presentation. Also, Y. Sun helped in assembling some of the numerical data, and communications with E. Kaxiras, A. Paxton and V. Vitek were helpful in understanding some of the background in atomic calculations.

REFERENCES

ANDERSON, P. M. 1986 Ph.D. thesis, Division of Applied Sciences, Harvard University, Cambridge, MA.

ARGON, A. S. 1987 *Acta. metall.*, **35,** 185.

ARMSTRONG, R. W. 1966 *Mater. Sci. Engng* **1,** 251.

ASHCROFT, N. W. and MERMIN, N. D. 1976 *Solid State Physics.* Holt, Rinehart & Winston, New York.

BARNETT, D. and ASARO, R. J. 1972 *J. Mech. Phys. Solids* **20,** 353.

BELTZ, G. E. and RICE, J. R. 1991a In *Modeling the Deformation of Crystalline Solids: Physical Theory, Application, and Experimental Comparisons* (edited by T. C. LOWE and A. ROLLETT). ASM/AIME (in press).

BELTZ, G. E. and RICE, J. R. 1991b Manuscript submitted to *Acta metall. mater.*

BRANDES, E. A. 1983 *Smithells Metals Reference Book*, 6th edition. Butterworths, London.

CHEUNG, K. 1990 Ph.D. thesis, Department of Nuclear Engineering, MIT, Cambridge, MA.

CHEUNG, K., YIP, S. and ARGON, A. S. 1991 *J. appl. Phys.* **69,** 2088.

DAW, M. S. and BASKES, M. I. 1984 *Phys. Rev. B* **29,** 6443.

DRAGONE, T. L. and NIX, W. D. 1988 *Scr. metall.* **22,** 431.

DUESBERY, M. S., MICHEL, D. J., KAXIRAS, E. and JOOS, B. 1991 In *Defects in Materials* (edited by P. D. BRISTOWE, J. E. EPPERSON. J. E. GRIFFITH and Z. LILIENTAL-WEBER), Vol. 209, p. 125. Materials Research Society.

ESHELBY, J. D. 1970 In *Inelastic Behavior of Solids* (edited by M. F. KANNINEN, W. F. ADLER, A. R. ROSENFIELD and R. I. JAFFEE), p. 77. McGraw-Hill, New York.

FOILES, S. M., BASKES, M. I. and DAW, M. S. 1986 *Phys. Rev. B* **33,** 7983.

FOILES, S. M. and DAW, M. S. 1987 *J. Mater. Res.* **2,** 5.

HIRTH, J. P. and LOTHE, J. 1968 *Theory of Dislocations.* McGraw Hill, New York.

HOAGLAND, R. G., DAW, M. S., FOILES, S. M. and BASKES, M. I. 1990 *J. Mater. Res.* **5,** 313.

KELLY, A., TYSON, W. R. and COTTRELL, A. H.	1967	*Phil. Mag.* **15,** 567.
LIN, I.-H. and THOMSON, R.	1986	*Acta metall.* **34,** 187.
NABARRO, F. R. N.	1947	*Proc. phys. Soc.* **59,** 256.
PAXTON, A. T., GUMBSCH, P. and METHFESSEL, M.	1991	*Phil. Mag. Lett.* **63,** 267.
PEIERLS, R. E.	1940	*Proc. phys. Soc.* **52,** 34.
RICE, J. R.	1968a	*J. appl. Mech.* **35,** 379.
RICE, J. R.	1968b	*Fracture: an Advanced Treatise* (*Vol.* 2, *Mathematical Fundamentals*) (edited by H. LIEBOWITZ), Chap. 3, p. 191. Academic Press, New York.
RICE, J. R.	1987	In *Chemistry and Physics of Fracture* (edited by R. M. LATANISION and R. H. JONES), p. 23. Martinus Nijhoff, Dordrecht.
RICE, J. R. and THOMSON, R. M.	1974	*Phil. Mag.* **29,** 73
RICE, J. R. and WANG, J.-S.	1989	*Mater. Sci. Engng* **A107,** 23.
SCHOECK, G.	1991	*Phil. Mag.* **63,** 111.
STROH, A. H.	1958	*Phil. Mag.* **3,** 625.
SUN, Y., BELTZ, G. E. and RICE, J. R.	1991a	Research in progress on embedded atom models as a basis for estimation of normal stress effects in dislocation nucleation.
SUN, Y., RICE, J. R. and TRUSKINOVSKY, L.	1991b	In *High-temperature Ordered Intermetallic Alloys* (edited by L. A. JOHNSON, D. T. POPE and J. O. STIEGLER), Vol. 213, p. 243. Materials Research Society.
TYSON, W. R.	1975	*Can. metall. Q.* **14,** 307.
VITEK, V.	1968	*Phil. Mag.* **18,** 773.
VITEK, V., LEJCEK, L. and BOWEN, D. K.	1972	In *Interatomic Potentials and Simulation of Lattice Defects* (edited by P. C. GEHLEN, J. R. BEELER and R. I. JAFFEE), p. 493. Plenum Press, New York.
YAMAGUCHI, M., VITEK, V. and POPE, D.	1981	*Phil. Mag.* **43,** 1027.
WEERTMAN, J.	1981	*Phil. Mag.* **43,** 1103.
WILLIS, J. R.	1967	*J. Mech. Phys. Solids* **15,** 151.